TURBULENCE STUDIES OF THE FLOW OF DILUTE POLYMER SOLUTION ABOUT CIRCULAR CYLINDERS

Joel Rea Fitts

NAVAL POSTGRADUATE SCHOOL
Monterey, California

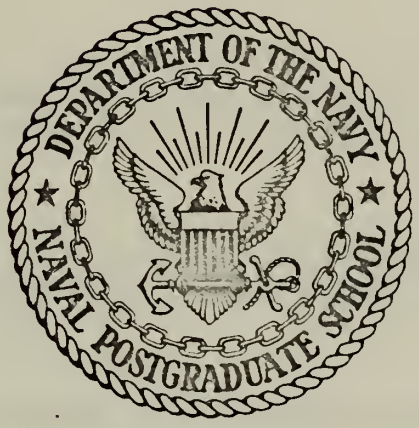

THESIS

TURBULENCE STUDIES OF THE FLOW
OF DILUTE POLYMER SOLUTION
ABOUT CIRCULAR CYLINDERS

by

Joel Rea Fitts

Thesis Advisor: Thomas Houlihan

June 1972

T148506

Approved for public release; distribution unlimited.

Turbulence Studies of the Flow of Dilute Polymer Solution about Circular Cylinders

by

Joel Rea Fitts
Lieutenant, United States Navy
B.E., Vanderbilt University, 1964

Submitted in partial fulfillment of the
requirements for the degree of

MASTER OF SCIENCE IN MECHANICAL ENGINEERING

from the

NAVAL POSTGRADUATE SCHOOL
June 1972

ABSTRACT

This study was a continuation of previous investigations of the flow of dilute (25 WPPM) polymer (Polyox WSR-301) solutions about bluff bodies in the drag transition flow regime. Detailed measurements of turbulence intensity, and turbulence microscale were taken in the near wake region of a circular cylinder for several degradation states of polymer flow. Additionally, the effects of polymer degradation upon hot-film anemometer operations were determined. The results of this study substantiated the determinations on turbulence indices in polymer flows which were previously reported.

TABLE OF CONTENTS

LIST OF FIGURES

I. INTRODUCTION

A. ORIENTATION

The subject of internal (pipe) flows of dilute polymer solutions has received a great deal of attention in the last decade. It is a well established fact that such polymer solutions exhibit larger flow rates than those of pure solvent (water) in analogous flow systems. Several authors have shown that the introduction of polymers into turbulent internal flow fields "suppresses" turbulence intensity throughout the flow [1-4]. More specifically, in pipe flows the polymer solution thickens the laminar sublayer and decreases the wall velocity gradient thus reducing the wall shear stress forces. Ultimately, larger flow rates result for polymer solutions under a pressure gradient equal to that existent in the pipe flow of a pure solvent. Thus the introduction of polymers leads to a beneficial result by causing an internal flow field to become less turbulent.

In stark contrast, considering an external flow about a bluff body, classical results show that the drag coefficient of the body will be reduced only if the flow field becomes more turbulent. Hence, if polymers are to have beneficial effects in external flows, they must somehow augment flow field turbulence. This anamolus behavior of polymers in solution, i.e., the enhancement of turbulence effects in

external flows, was the subject of three previous investigations [5-7] at NPS.

Sarpkaya and Rainey [5] studied the integrated effects of the flow of dilute polymer solutions about circular cylinders. In degraded polymer solutions, they noted a "premature" transition occurring at well defined flow conditions.

In tap water, this transition from a laminar to a turbulent state occurred at a specific Reynolds Number in accordance with classical results. The flow about the circular cylinders in a polymer solution experienced a characteristically similar transition but at a lower Reynolds Number. The polymer, in effect, acted like a tripping mechanism in the flow field.

Kell [6] studied surface pressure fluctuations on a circular cylinder in polymer flow. From his results he concluded that fundamental vortex shedding frequencies were not altered in polymer solutions from those occurring in water at the same Reynolds Number. However, the amplitudes of the surface pressure fluctuations recorded were decreased throughout the entire range of the measured frequency spectra.

Schimmels [7] investigated the intensities and the frequency spectra of turbulent polymer flows in the near wake region of a one-inch circular cylinder. He found that turbulence intensities in polymer flows were greatly enhanced in the wake core area compared to those recorded in tap water. In general, the enhancement was a function of

polymer degradation state and Reynolds Number. The polymer in solution acted to compress the cylinder wake core and to increase the turbulence intensities occurring therein.

B. OBJECTIVES OF THE EXPERIMENT

The present study was concerned with measurements of turbulence intensity, turbulence microscale, and turbulence macroscale in the near wake region of a circular cylinder for several degradation states of polymer flow. The studies were conducted at the Reynolds Number range before, during and after the drag crisis region observed by Sarpkaya and Rainey [5]. Additionally, the effects of polymer additives upon hot-film anemometer operations were investigated in detail.

C. DEFINITION OF MEASURED QUANTITIES

1. Turbulence Intensity

Turbulence Intensity,I, is related to anemometer voltage readings in the following manner:

$$I = \frac{u'}{\bar{U}} = \frac{4 \times \bar{V} \times e'}{\bar{V}^2 - \bar{V}_0^2}$$

where u' is the root-mean-square value of the fluctuating component of the flow velocity, $\bar{U}$ is the mean value of the flow velocity, $\bar{V}$ is the hot-film sensor D.C. level, e' is the root-mean-square value of the fluctuating component of the sensor signal, and $\bar{V}_0$ is the extrapolated zero flow value of the sensor voltage. This expression is developed

in detail in the Appendix.

Turbulence relationships are derived from the fundamental anemometer calibration equation:

$$\bar{V}^2 = \bar{V}_0^2 + B\sqrt{\bar{U}}$$

where $\bar{V}$ is the voltage across the sensor, $\bar{V}_0$ is the extrapolated zero flow voltage and B is a constant, which is the slope of the calibration curve. In the present experiments, $\bar{U}$ was determined by a pitot-static arrangement consisting of a pressure tap in the test cylinder at the stagnation point and a static tap located five diameters upstream of the test cylinder in the sidewall of the test section. The experimenter was cognizant of the questionable use of a pitot-static tube for velocity measurements in non-Newtonian fluids [1-4]. However, the studies of Friehe and Schwarz [8] have shown that except for small tubes (on the order of one cm. diameter) no discrepancies arise in velocity measurements in polymer solutions using regular pilot-static arrangements.

Thus, the velocities determined by the pilot-static test arrangement in calibration runs were assumed to be true. Hence the effects noted in these tests did indeed arise from hot-film sensor operations and not from pitot-static measurement discrepancies.

2. Turbulence Microscale

As described by Hinze [8], the turbulence microscale is a measure of the average dimension of the smallest eddies in a flow field. These smallest eddies are responsible for the dissipation of flow kinetic energy into heat. In the present studies, microscale profiles in tap water were compared to those of polymer solutions at various degradation states of the polymer solutions for a range of Reynolds Numbers.

The equation defining the longitudinal turbulance microscale is developed by Hinze from relationships involving longitudinal correlation coefficient.

Thus $$\frac{2}{\lambda_f^2} = -\left[\frac{\partial^2 f_1}{\lambda x_1^2}\right]_{x_1=0} = \frac{1}{u'^2}\overline{\left(\frac{\lambda u_1}{x_1}\right)^2}$$

where λ_f is defined as the longitudinal turbulence microscale, f is the longitudinal correlation coefficient, x_1 is a distance in the longitudinal direction, u' is the root-mean-square value of the fluctuating velocity and u_1 is the fluctuating component of the velocity in the longitudinal direction.

This last expression does not lend itself to easy experimental determination since the spatial gradient that appears is difficult to obtain. The interference effects of the sensor arrays necessary to accomplish the task prohibit accurate determinations. By making use of Taylor's

hypothesis, i.e., $\partial/\partial t = -\bar{U}\partial/\partial x$ which implies that in a turbulent flow where $\bar{U} >> u$, the turbulence pattern is swept along at the mean flow velocity, $\bar{U}$, an interchange of spatial and temporal derivatives can be affected.

The relationship for longitudinal microscale thus becomes:

$$\frac{2}{\lambda_f^2} = \frac{1}{u'^2\bar{U}^2} \overline{\left(\frac{\partial u_1}{\partial t}\right)^2}$$

In terms of sensor signals the microscale expression takes the following form:

$$\lambda_f = \frac{\sqrt{2} \times e' \times (\bar{V}^2 - V_0^2)^2}{B^2 \times \left(\frac{de}{dt}\right)'}$$

where $\bar{V}$ is the D.C. level of sensor signal in volts, e' is the root-mean-square of the fluctuating component of the sensor signal in volts, V_0 is the voltage across the sensor at zero flow velocity, B is the sensor sensitivity, and $\left(\frac{de}{dt}\right)'$ is the root-mean-square of the differentiated sensor signal. A complete derivation of this equation is contained in the Appendix. This investigation was concerned only with longitudinal turbulence microscale measurement.

3. Turbulence Macroscale

The turbulence macroscale is a measure of the longest connection, or correlation, between the velocities at two points of the flow field [8].

Measurement of velocities at two points in the flow field requires sensors at both places. With this arrangement there is always the possibility of the upstream sensor affecting the flow past the downstream sensor. This fact, coupled with the trouble that was experienced with the hot-film sensor at the outset of this study resulted in an attempt to determine an Eulerian correlation which requires the operation of a single hot-film sensor.

The relationship between the turbulence macroscale correlation and the Eulerian correlation is developed in the Appendix. The basis for the relationship is again that of Taylor's hypothesis [8].

II. EQUIPMENT AND PROCEDURE

A. EQUIPMENT

1. NPS Water Tunnel

The experiments were performed in the NPS water tunnel [5-7]. Minor alterations to effect more efficient deaerating were incorporated.

2. Test Specimen

A one inch diameter circular cylinder was used in all tests. The method of mounting the cylinder and the location of pitot-static pressure tap was unchanged from that reported in previous studies.

3. Sensor and Sensor Support

It was intended to utilize available Thermo Systems Incorporated (TSI) conical hot-film sensors (Model 1231W) for all experiments. After two failures of this type sensor, a DISA conical sensor (Model 55A87) (Fig. 1) was introduced to measure the fluctuating and mean components of velocity in the longitudinal direction. The sensor support was a 1/4 inch stainless steel tube with an integral brass splitter plate. The placement of the sensor in the test section was similar to that described by Schimmels [7]. The bulk of data was taken at the + 2.5 X/D port, i.e., 2 1/2 cylinder diameters downstream of the cylinder (Fig. 2).

Additionally, a final check of turbulence intensity and turbulence microscale data was completed at the + 1.5

X/D location in both tap water and polymer solutions for a Reynolds Number of 80,000 with a TSI (Model 1231W) conical hot-film sensor.

4. Sensor Operations

Each of the TSI sensors failed after calibration and water data runs. Their individual lifetimes were less than five hours each. The DISA sensor that was used to record the + 2.5 X/D data failed after 21 hours of operation. The sensors signaled impending failure in the following manner. First,the cold resistance of the sensor increased. A small increase in resistance is normal due to the hardening and aging of the sensitive platinum filament. However, a large increase in resistance over a short time span was a sure indication that failure was imminent.

With a constant overhead setting (nominally 1.05 to 1.10), increasing sensor resistance caused a decline in sensitivity and frequency response. Unit frequency response was able to be reset by adjusting the bridge amplifier gain (trim) and feedback circuit components (stability) of the anemometer. However, a point was reached beyond which no amount of adjustment would result in an acceptable frequency response. The sensor was then judged to be no longer of any value and replacement was deemed necessary.

Frequency response could also be reset by increasing the sensor overheat ratio. However, this procedure merely quickened decay by increasing the heating of the sensor filament. As a result of the foregoing considerations, a

fast check of the operational state of a unit was made by noting the sensor D.C. voltage under quiescent conditions. If this voltage did not remain within 0.1 volt from one run to another, a change in sensor activity was denoted since the temperature sensitivity of hot-film sensors is normally negligible.

5. Instrumentation

Differential pressure measurements were recorded in the manner reported by Schimmels [7]. A TSI Constant Temperature-Type Anemometer (Model 1050) was operated with the two hot-film sensors utilized - a DISA (55A87) conical sensor and a TSI (1231W) right angle conical sensor. The anemometer unit was set at an overhead ratio of 1.05 to provide a response band of 0-2,000 Hz. The output of the anemometer was paralled to a Simpson digital voltmeter (Model 2700), a TSI RMS Voltmeter (Model 1060) with a ten second time constant, and a TSI Correlator (Model 1015C) which was used to differentiate the sensor signal with respect to time. The Simpson digital voltmeter provided the D.C. level of sensor signal; the TSI RMS voltmeter provided the RMS value of the fluctuating component. The TSI Correlator (in the differentiator mode) fed the differentiated sensor signal (multiplied by a one millisecond time constant) to a second TSI RMS Voltmeter (Model 1060) for turbulence microscale determinations. The fluctuating signal and the differentiated sensor signal were continuously monitored on a Textronics dual trace oscilloscope (Model 531).

A schematic of this system is presented in Fig. 2.

Macroscale data was obtained by feeding the anemometer signal to a Princeton Applied Research Corporation Model 101 Correlation Function Computer (hereafter referred to as the PAR Correlator). The PAR Correlator output was paralleled to the Textronics oscilloscope and a Hewlett-Packard Model 135 X-Y plotter (Fig. 3).

In the fast readout mode the PAR Correlator displayed measured correlograms on the oscilloscope face. The oscilloscope trace continued to grow in magnitude as long as the PAR Correlator remained in the fast readout mode. Thus, scope photography was unsatisfactory with slow speed film that required long exposure times. In all readout modes except the fast mode, the oscilloscope trace did not appear continuously but only as a pulse response when the PAR Correlator began a new sample.

With the PAR Correlator in the slow or medium readout mode the parallel X-Y plotter was completely controlled by the PAR Correlator. In the slow readout mode, at the completion of a trace the pen returned to the abscissa and returned to the origin along this axis. At the origin, the pen deflected to an initial ordinate value and proceeded to plot another correlogram. In the medium readout mode the pen did not return on the abscissa but deflected upwards about half way through its return to the origin. Since correlation displays were obtained more rapidly in the medium readout mode than in the slow readout mode, the

following procedure was established for recording correlograms. The medium readout mode was utilized until the pen was approximately 1/2 inch from the end of a correlogram trace. The slow readout mode was then switched in. Subsequently, the pen would trace out a base abscissa on its return and thus there was no need to closely align the pen prior to making a record.

B. PROCEDURE

1. Solution Characteristics

The degradation state of the polymer solution was characterized by the Percent Pipe Drag Reduction (PDR). The PDR represents the reduction of the drag in polymer solution from that of water in turbulent pipe flow. Operation of the rheometer apparatus for determination of the degradation state of the polymer (i.e. for calculation of the PDR value) was identical to that reported in earlier studies at NPS. Likewise, the Polyox WSR-301 polymer additive was identical to that used in these previous investigations.

2. Preparation of Test Fluid

The tap water in the tunnel (500 gallons) was filtered through a Cuno (Model PE 1B2) filter in excess of eight hours prior to adding any polymer. The tunnel level was then lowered to the mid point of the test section, with the drawn-off filtered tunnel water being held in an adjoining stainless steel storage tank. A slow flow through

the tunnel was then initiated. Dry polymer was slowly sprinkled into the flowing solvent downstream of the cylinder for approximately five minutes time to reduce any chance of coagulation during mixing. The tunnel pump was then shut down.

To reduce the amount of entrained air that the subsequent refilling procedure invariably introduced, the water from the storage tank was returned through the tunnel filter unit. A compromise between longer refilling times and the amount of entrained air was struck by adjusting the supply valve to the filter unit to obtain about 15 psig head on the storage tank pump.

A quick release shut-off valve was placed in the air bleed line at the downstream high point of the water tunnel. It was observed that concentrated polymer solution would be drawn into the air bleed line as the water tunnel was being refilled after the mixing procedure was completed. Closing the shut-off valve solved the problem.

After the polymer had aged approximately 24 hours, the polymer solution was ready for testing. Entrained air was removed by opening the air bleed line valve and by starting and stopping the tunnel intermittently until the air was removed.

3. Tunnel Characteristics

Tunnel Correction Factors were calculated in the same manner as previously reported. They ranged in magnitude from 1.0754 for high PDR values at an 80,000 Reynolds

Number to 1.044 for low PDR values at a 140,000 Reynolds Number.

The tunnel coordinate axes used in the investigation are defined in Figure 4.

4. Sensor Calibration as a Function of Pipe Drag Reduction

A calibration curve was first obtained in filtered tap water. A polymer solution (25 WPPM) was then mixed and aged. Beginning with a high PDR and working down to lower PDR's calibration curves were obtained for several degradation state.

5. Measurement of Turbulence Intensity and Turbulence Microscale

Measurements of turbulence intensity and microscale values in water flows and polymer flows in the wake of a one-inch diameter cylinder were recorded at Reynolds Numbers of 80,000, 100,000, 120,000 and 140,000. Traverses of the flow field were made at downstream positions of +1.5 X/D and +2.5 X/D at 11 and 15 stations, respectively, between the +2.5 Y/DIAM and 0.0 Y/D locations. At each Y/D station $\overline{V}$, e' and $(\frac{de}{dt})'$ were recorded. The turbulence intensity and the turbulence microscale were computed and their profiles drawn by the NPS IBM 360 computer.

Preliminary investigation disclosed that the profiles below the cylinder were symmetric and that additional traversing below the center line of the cylinder would not produce any more significant data.

The regular ordinate spacing in data taking was one-quarter inch. However, this spacing was reduced to one-eighth inch in areas of rapid change in sensor signal such as those occurring in the shear layer.

6. Measurement of the Turbulence Macroscale

Turbulence macroscale measurements were attempted at an X-Axis position of +2.5 X/D. Tap Water measurements were recorded at Reynolds Numbers of 80,000, 100,000, 120,000, and 120,000 at four Y/D locations (+0.0, +0.5, +1.0 and +1.5 Y/D). Polymer solution measurements were likewise attempted at the same Y/D locations for a Reynolds Number of 80,000. Unfortunately the predominant periodic nature of the near wake region was undiminished even at the +2.5 X/D station. Hence, no conclusive macroscale values were determined. Figure 40 is typical of the correlograms obtained.

III. PRESENTATION OF DATA

A. EVALUATION OF EXPERIMENTAL ERRORS

Since the experimental apparatus utilized was, except for the sensor, identical to that reported by Schimmels [7], the experimental errors were determined to be of the same order of magnitude. For turbulence intensity determinations, the error equalled 3% outside the wake core and 6% within the wake core. The overall error in turbulence microscale determination reached 15% in value.

B. CALIBRATION OF THE HOT-FILM SENSOR AS A FUNCTION OF POLYMER DEGRADATION

The records obtained in the DISA and TSI hot-film calibration runs are presented in Figures 5 and 6. The curves for the various PDR's and the tap water curve all have the same slope in the case of the DISA sensor. The slopes of the various PDR's for the TSI sensor varied slightly, but subsequent calculations involving an average slope are well within the degree of accuracy (10%) required for turbulence evaluations. In both cases, the highest PDR curve had a larger zero flow intercept than water. The subsequent lower PDR curves converge to that of water with the exception of the lowest PDR curve which fell below the water curve. The anamolus behavior of this last curve remains puzzling.

C. MEASUREMENT OF THE TURBULENCE INTENSITY AND THE TURBULENCE MICROSCALE

Figures 7 through 14 present the intensity and microscale profiles in tap water and in selected polymer solution degradation states for each Reynolds Number tested. Figures 15 through 25 present the microscale profiles of the respective polymer solution degradations states and tap water individually since on the 80,000, 100,000, and 120,000 Reynolds Numbers composite graphs it becomes difficult to select an individual polymer solution degradation value. Figures 26 and 27 present the intensity and microscale profiles of tap water and selected polymer solution degradations at the +1.5 X/D location at the 80,000 Reynolds Number.

The general trend of the intensity profiles is the same as that reported by Schimmels [7].

At the +2.5 X/D station the width of the wake core is larger than that of the 1.5 X/D and 1.0 X/D stations, indicating that the core region is still growing. However, the magnitudes of the turbulence intensities at this station, both within and outside the core region, are within 10% of those reported at the previous locations.

Outside the core, the turbulence intensities measured in polymer solution are suppressed below that of water for each Reynolds Number. Inside the core, just the opposite state of affairs exists, i.e., the turbulence intensities in polymer solutions are enhanced with respect to those in

water. For each Reynolds Number, a minimum intensity is reached at a certain PDR, generally around 20%, and for PDR's less than this value the intensity value snaps back toward that of tap water.

The comparison between previously reported intensity data [7] and that obtained in this study at +1.5 X/D (Figs. 28 through 37) was excellent. Outside the wake core the differences noted were less than 5% at any PDR value. Inside the wake core the difference in turbulence levels were less than 20%. Thus, even within wake core where turbulence intensities are of such a magnitude as to have no linear meaning, the correspondence between check runs is within nominal turbulence variances. Realizing that the sensor utilized in this study was ten time more sensitive than that used in previously recording data at this station [7], this correspondence is even the more remarkable.

The maxima in the turbulence microscale profiles can be considered quantitative indicators of wake core size. This tip of the "nose" of the profiles corresponds to the edge of wake, i.e., where spikes in intensity oscilloscope traces are noticed. This "nose" was seen to move to lower and lower Y/D values as the polymer solutions degraded. When viewed at a specific Y/D value the polymer solution curves indicated that large reductions in microscale - approaching 80% in some cases occur. When viewed "nose-to-nose", i.e., in a manner using the edges of the wake cores observed both

in tap water and polymer solutions as reference points, (Figs. 38 and 39) the reduction in microscale is realized as being consistent in character throughout the flow field behind the cylinder.

IV. DISCUSSION OF RESULTS AND CONCLUSIONS

A. SENSOR CALIBRATION AS A FUNCTION OF POLYMER DEGRADATION

The calibration curves for the two hot-film sensors obtained indicated that the effects of degradation (PDR value) of a dilute polymer solution (25 WPPM) on turbulence measurements are not significant. It was noted that the slopes of the calibration curves evidenced were nearly equal and that the zero flow voltage value converged to that of water (except for the lowest PDR) as the polymer solution degraded. Maximum differences between intensity values and microscale values calculated using both average and exact values of slopes and zero flow voltages were evaluated to be 3% and 7% respectively. Since difference in reported turbulence values of 10% are acceptable, the effects of degradation upon sensor operations are realized as being negligible.

B. TURBULENCE INTENSITY MEASUREMENTS

A complete verification of turbulence intensity measurements in the wake flow of dilute polymer solutions about a circular cylinder has been accomplished using sensors that varied in sensitivity by a factor of ten. Differences in turbulence intensity obtained were less than 5% outside the wake core for any particular degradation state of polymer. Inside the wake core the maximum evaluated difference was 20%. Moreover, the overall character of all

of the intensity profiles measured by these vastly different sensors was remarkably consistent. This leads to a high confidence level in the turbulence measurements reported.

C. TURBULENCE MICROSCALE MEASUREMENTS

The maximum value of the turbulence microscale profile was determined to be an indication of the location of the edge of the cylinder wake core. Thus, using this criterion, the compression of the cylinder wake by the addition of polymers can be more accurately portrayed. Reductions of microscale values approaching 80% in magnitude have been noted in this regard. Another comparison of polymer effects upon turbulence indicies can be affected by aligning the tips of the microscale profiles as reference points. When compared in this manner the microscale profiles show that the water and polymer flows are, except for the decreased amplitudes, existent in the polymer solutions, quite similar in overall characteristics.

APPENDIX

Turbulance Intensity Relationship

From the calibration equation

$$V^2 = V_0^2 + B\sqrt{U}$$

differentiating with respect to time gives

$$2V \frac{dV}{dt} = \frac{B \frac{dU}{dt}}{2\sqrt{U}} \quad .$$

Letting: $\frac{dV}{dt} = e \; ; \quad \frac{dU}{dt} = u \; .$

Then

$$2V\, e = \frac{B\, u}{2\sqrt{U}}$$

or

$$\frac{u}{\sqrt{U}} = \frac{4 \times V \times e}{B}$$

Multiplying both sides of this equation by $\frac{1}{U}$ gives:

$$\frac{u}{\bar{U}} = \frac{4 \times V \times e}{B\sqrt{U}}$$

From the calibration equation

$$B\sqrt{U} = V^2 - V_0^2 \; .$$

Therefore

$$\frac{u}{\bar{U}} = \frac{4 \times V \times e}{(V^2 - V_0^2)}$$

and

$$\frac{u'}{\bar{U}} = \frac{4 \times \bar{V} \times e'}{(\bar{V}^2 - V_0^2)}$$

where:

$\bar{V}$ = D.C. Level of sensor signal.

e' = RMS of the fluctuating component of sensor signal.

V_0 = Extrapolated value of the zero flow sensor D.C. level.

$\frac{u'}{\bar{U}}$ = Turbulence Intensity (%)

Turbulence Microscale Relationship

From Hinze, the turbulence microscale is defined by the relation:

$$\frac{2}{\lambda_f^2} = \frac{1}{u'^2} \overline{\left(\frac{\partial u}{\partial x}\right)^2} \quad .$$

Applying Taylor's Hypothesis, $\frac{\partial}{\partial t} = -\bar{U} \frac{\partial}{\partial x}$, in this equation give:

$$\frac{2}{\lambda_f^2} = \frac{1}{\bar{U}^2 u'^2} \overline{\left(\frac{\partial u}{\partial t}\right)^2} \quad . \qquad (1)$$

Rearranging and solving for λ_f yields

$$\lambda_f = \frac{\sqrt{2}\, u'\, \bar{U}}{\sqrt{\overline{\left(\frac{\partial u}{\partial t}\right)^2}}} = \frac{\sqrt{2}\, u'\, \bar{U}}{\left(\frac{\partial u}{\partial t}\right)'} \qquad (2)$$

Using the equation derived for Turbulence Intensity

$$\frac{u'}{\bar{U}} = \frac{4 \times V \times e'}{(V^2 - V_0^2)}$$

and multiplying by $\bar{U}^2$ gives:

$$u'\, \bar{U} = \frac{4 \bar{V}\, \bar{U}^2\, e'}{(V^2 - V_0^2)} \quad . \qquad (3)$$

Differentiating the Fluctuation Equation

$$\frac{u}{\bar{U}} = \frac{4 \times \bar{V} \times e}{(V^2 - V_0^2}$$

with respect to time yields:

$$\frac{du}{dt}\ \frac{1}{\bar{U}} = \frac{4\ \bar{V}}{(V^2-V_0^2)}\ \frac{de}{dt}$$

$$\left(\frac{du}{dt}\right)' = \frac{4\ x\ \bar{V}\ x\ \bar{U}}{(V^2 - V_0^2)}\ \left(\frac{de}{dt}\right)' \quad . \quad (4)$$

Substituting equations (3) and (4) into equation (2) gives:

$$\lambda_f = \frac{\sqrt{2}\ \frac{4\bar{V}\ \bar{U}^2\ e'}{(V^2 - V_0^2)}}{\frac{4\bar{V}\ \bar{U}}{(V^2 - V_0^2)}\left(\frac{de}{dt}\right)'}$$

$$\lambda_f = \frac{2\ \bar{U}\ e'}{\left(\frac{de}{dt}\right)'}$$

From the calibration equation

$$\bar{U} = \frac{(\bar{V}^2 - V_0^2)^2}{B^2}$$

Thus

$$\lambda_f = \frac{\sqrt{2}\ (\bar{V}^2 - V_0^2)^2\ \ e'}{B^2\ \left(\frac{de}{dt}\right)'} \qquad \text{QED}$$

where:

e' = RMS value of the fluctuating component [volts].

$\bar{V}$ = D.C. level of sensor signal [volts].

V_0 = The extrapolated value of the zero flow sensor [volts].

$\left(\frac{de}{dt}\right)'$ = RMS value of the differentiated sensor signal $\left[\frac{\text{Volts}}{\text{Sec}}\right]$.

B = The slope of the sensor calibration curve $\left[\frac{\text{volts}^2}{\sqrt{\frac{\text{ft}}{\text{sec}}}}\right]$.

λ_f = Turbulence Microscale [ft].

Measurement of Turbulence Macroscale

From Hinze, the Turbulence Macroscale is defined by the relation

$$\Lambda_f = \int_0^\infty f(x)\, dx$$

where

where $f(x) = \dfrac{\overline{u(1)\ u(1+x)}}{u'^2}$ is the longitudinal correlation coefficient. Incorporating Taylor's Hypothesis gives

$$f(x) = R_E(\tau)$$

where $R_E(\tau) = \dfrac{\overline{u(t)\ u(t+\tau)}}{u'^2}$ is the Eulerian time correlation coefficient.

A relation between space and time follows from the incorporation of Taylor's Hypothesis into this development. Thus:

$$x = \bar{U}\tau \quad \text{and} \quad dx = \bar{U}\, d\tau.$$

Hence, $\Lambda_f = \bar{U} \int_0^\infty R_E(\tau)\, d(\tau)$.

It follows that a measurement of the temporal autocorrelation of a sensor signal, $R_E(\tau)$, can yield a value for turbulence macroscale.

A typical correlogram for decaying turbulence is portrayed below:

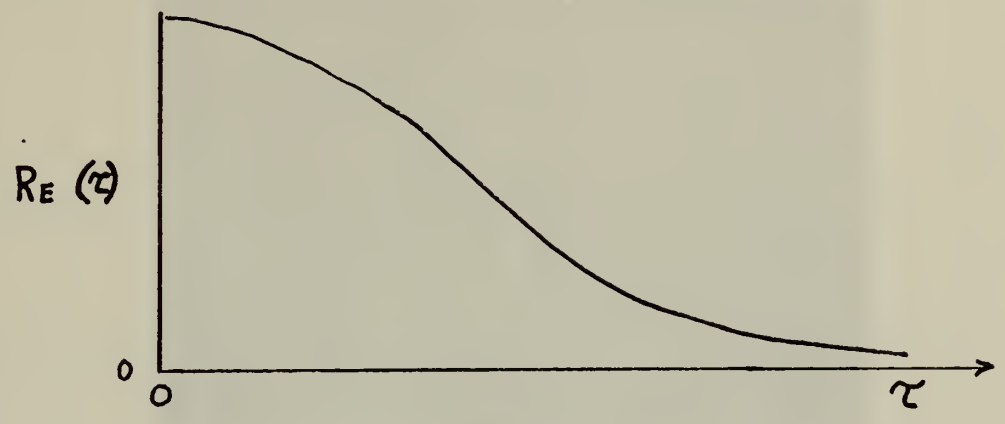

An evaluation of the integral $A = \int_0^\infty R_E(\tau)d\tau$ can be accomplished with a planimeter from this trace after a suitable $\tau \to 0$ value has been selected upon the record. Multiplication of this integral value by the mean flow velocity yields the longitudinal macroscale value, i.e., $\Lambda_f = \bar{U} A$. $R_E(\tau)$ is dimensionless whereas τ has the units of time. Hence the value of the integral, A, has the dimension of time. Since this integral value, A, is multiplied by the mean velocity, $\bar{U}$, to yield the value of the macroscale, Λ_f is seen to have the units of length.

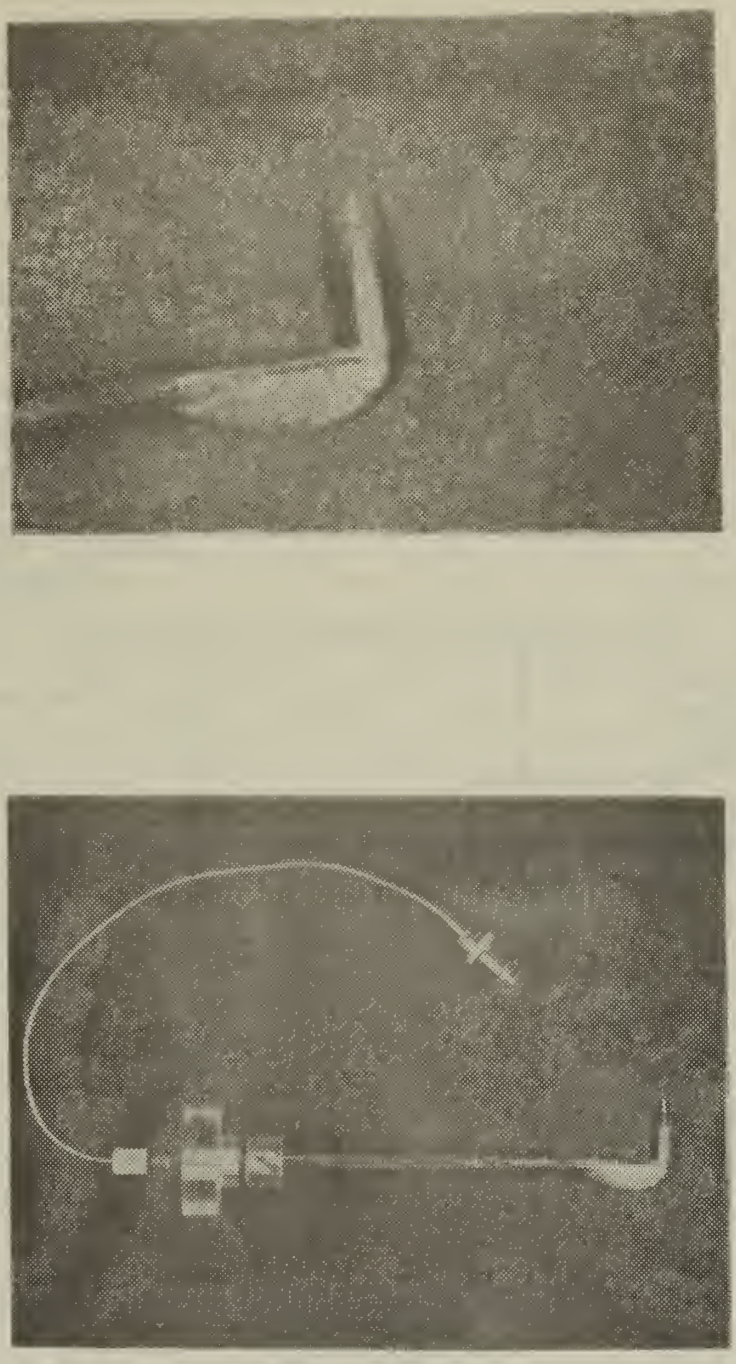

FIGURE 1: DISA CONICAL HOT-FILM SENSOR

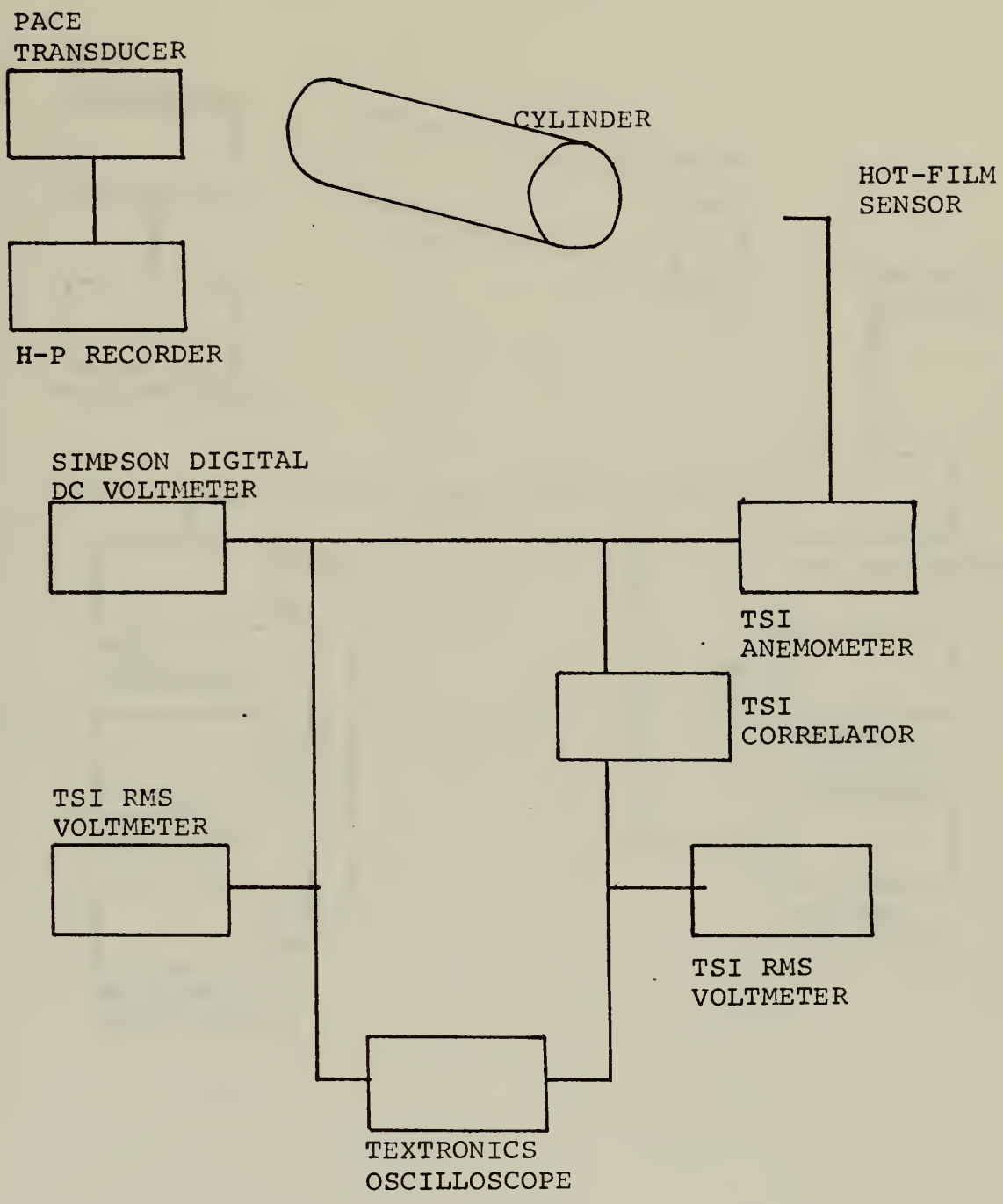

FIGURE 2: SCHEMATIC OF INSTRUMENTATION FOR TURBULENCE INTENSITY AND TURBULENCE MICROSCALE DETERMINATIONS

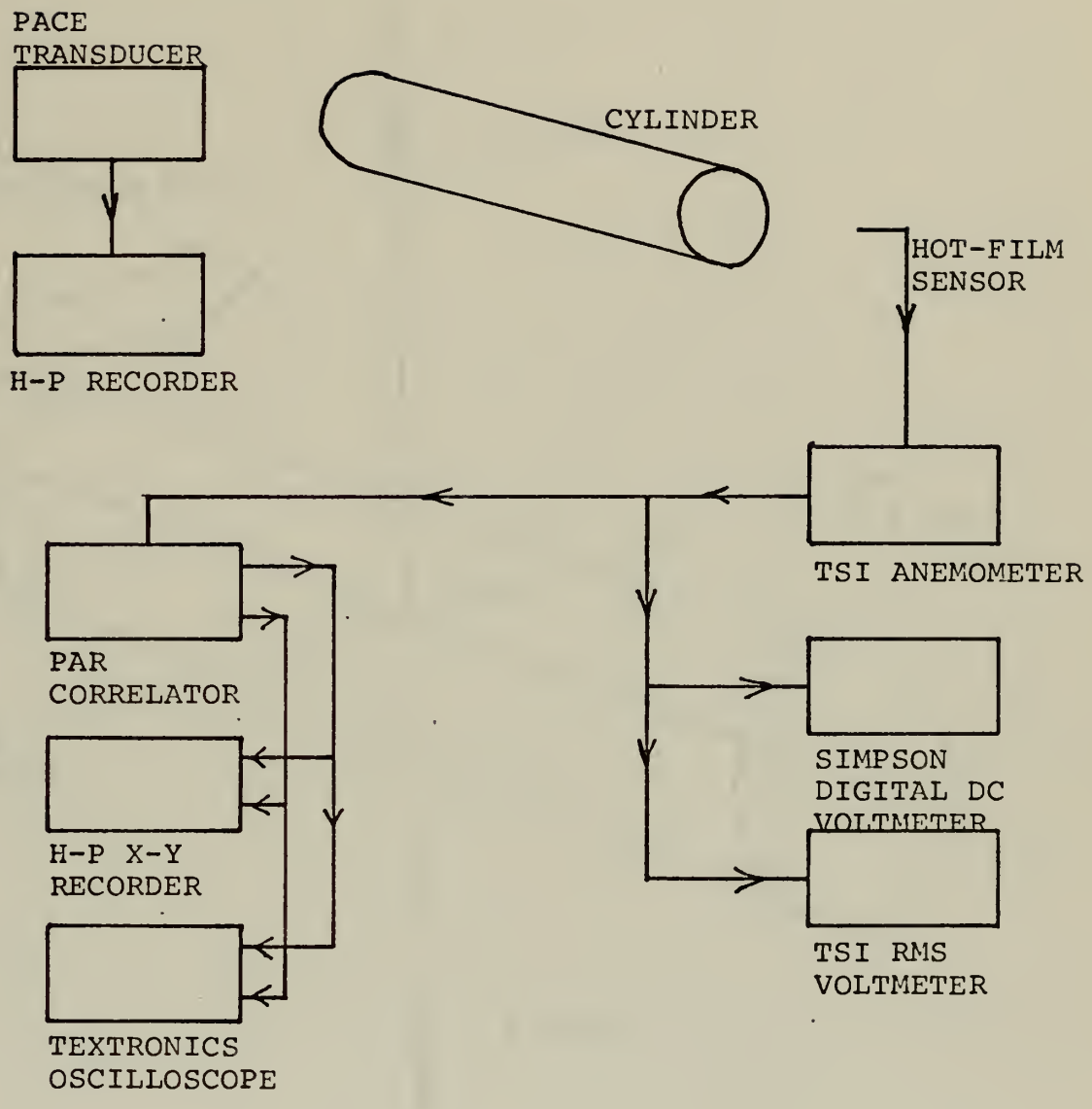

FIGURE 3: SCHEMATIC OF INSTRUMENTATION FOR MACROSCALE DETERMINATIONS

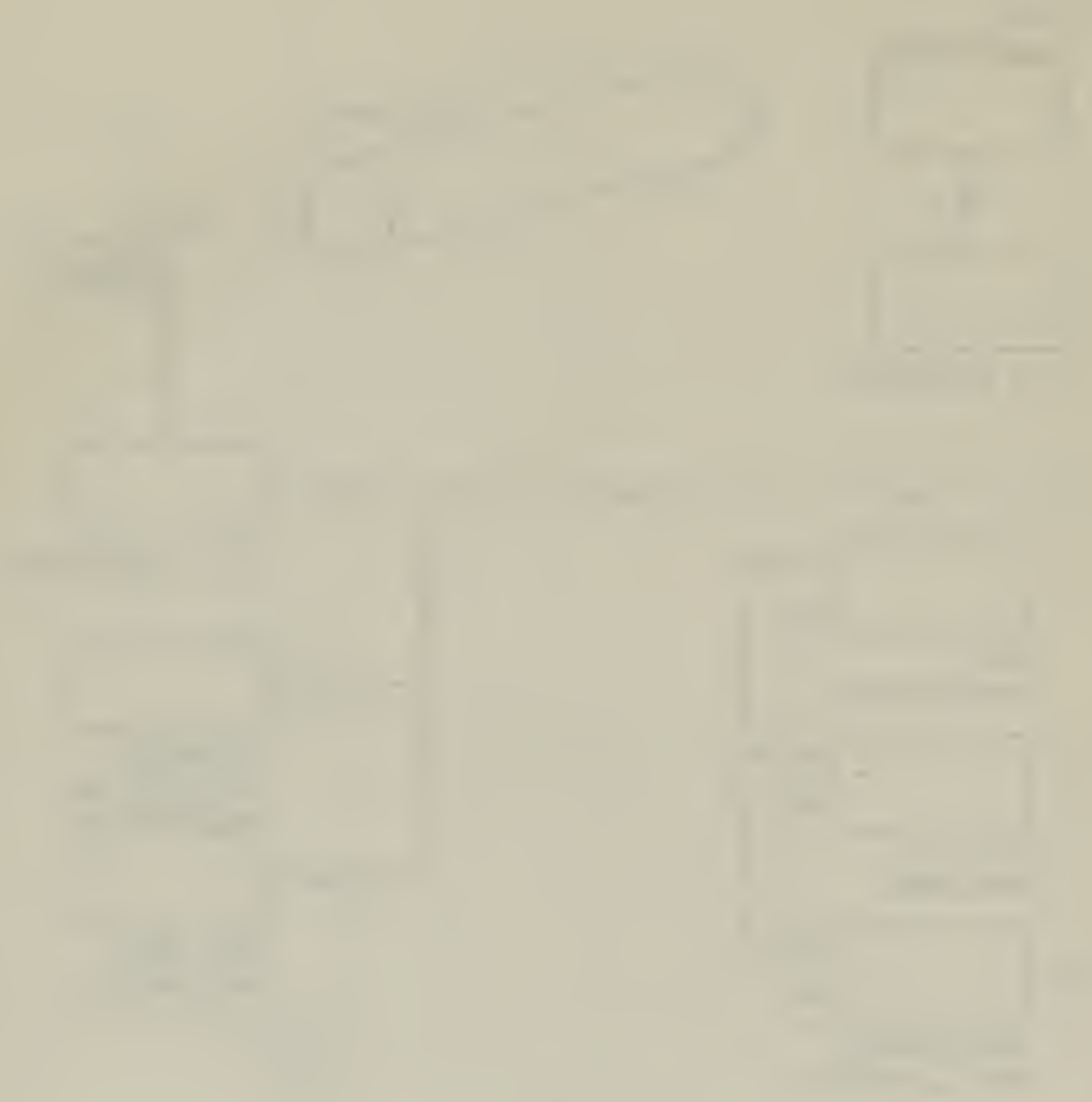

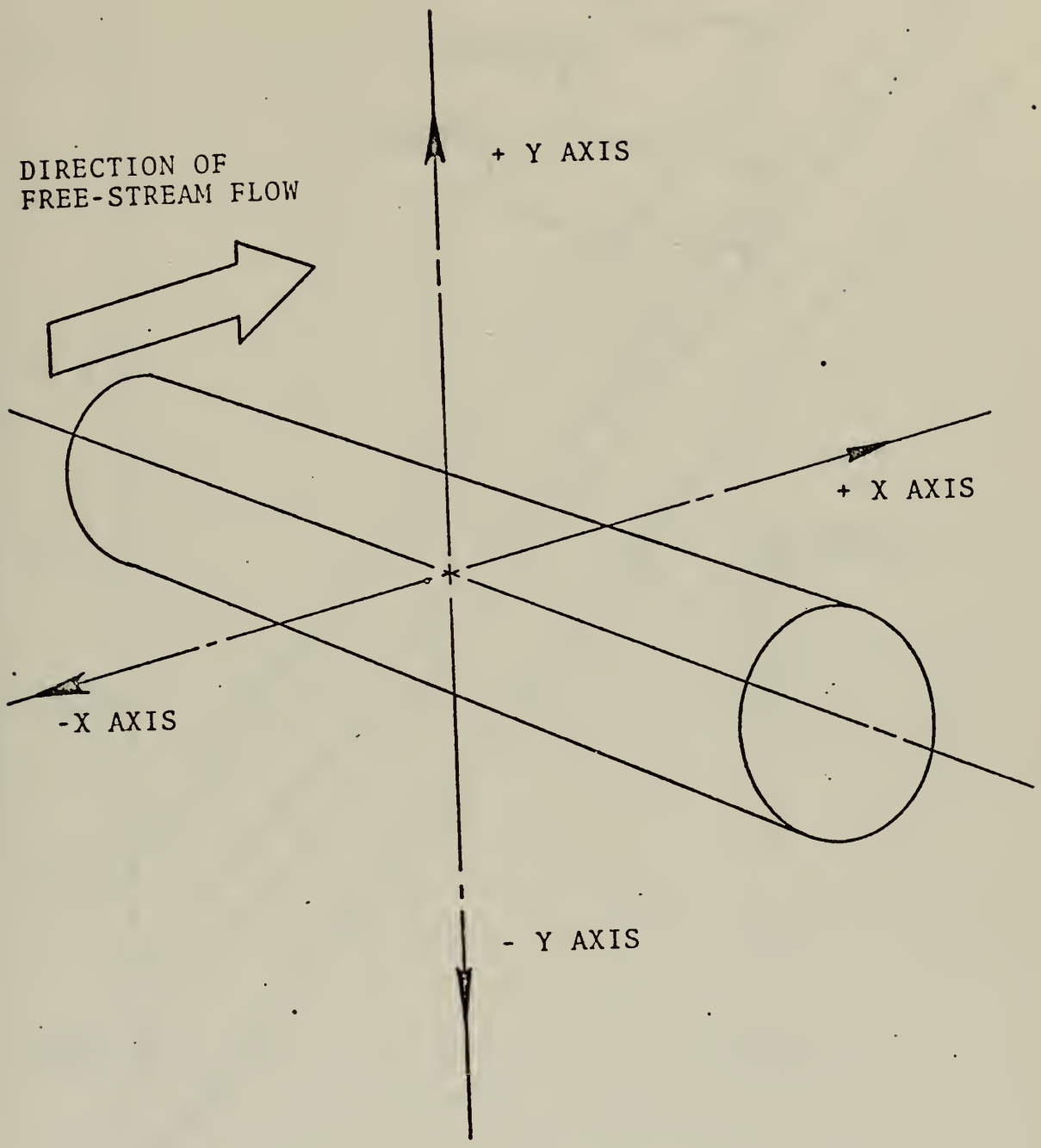

Figure 4 : DEFINITION OF COORDINATE AXES

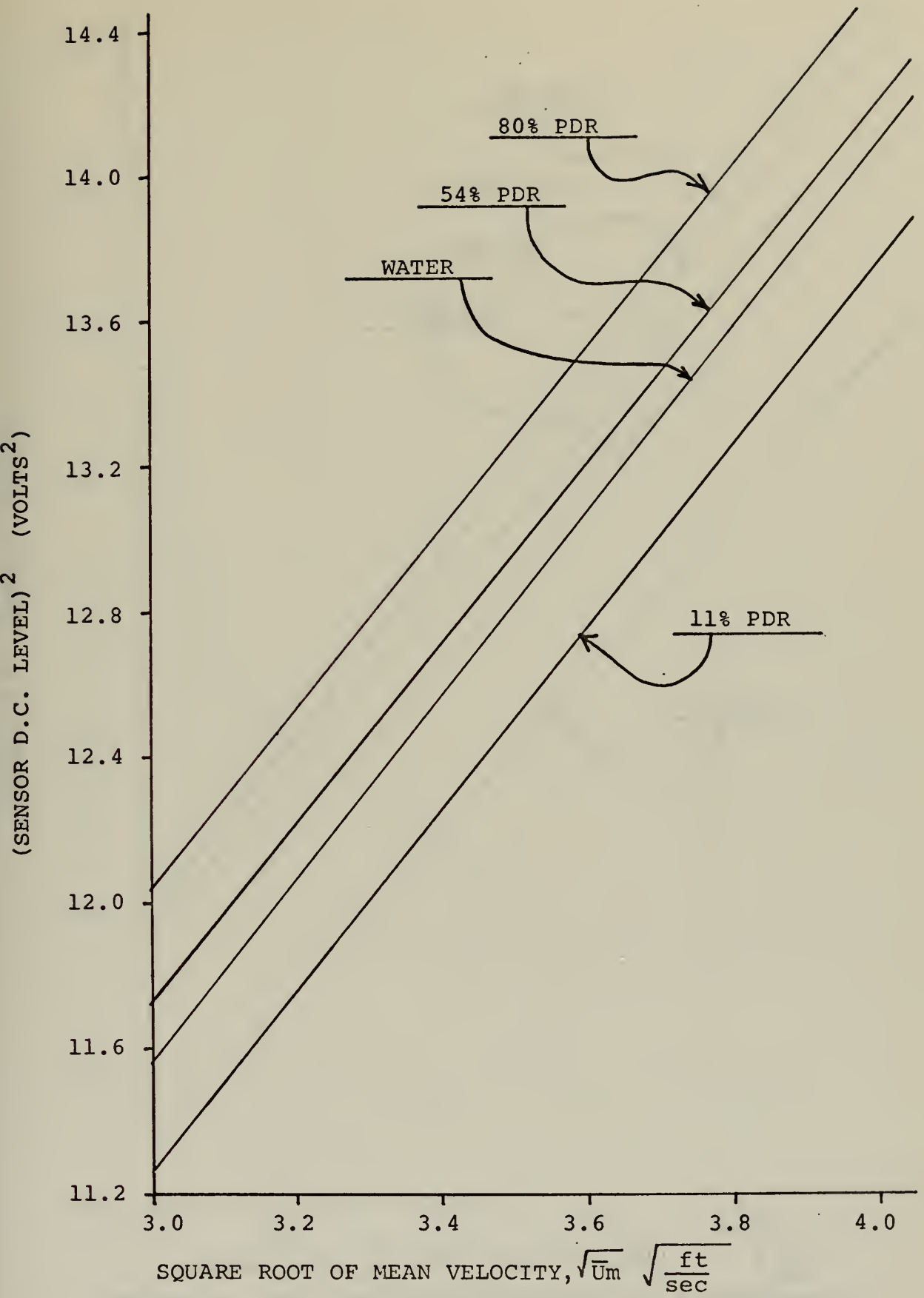

FIGURE 5: DISA HOT-FILM CALIBRATION AS A FUNCTION OF POLYMER SOLUTION DEGRADATION

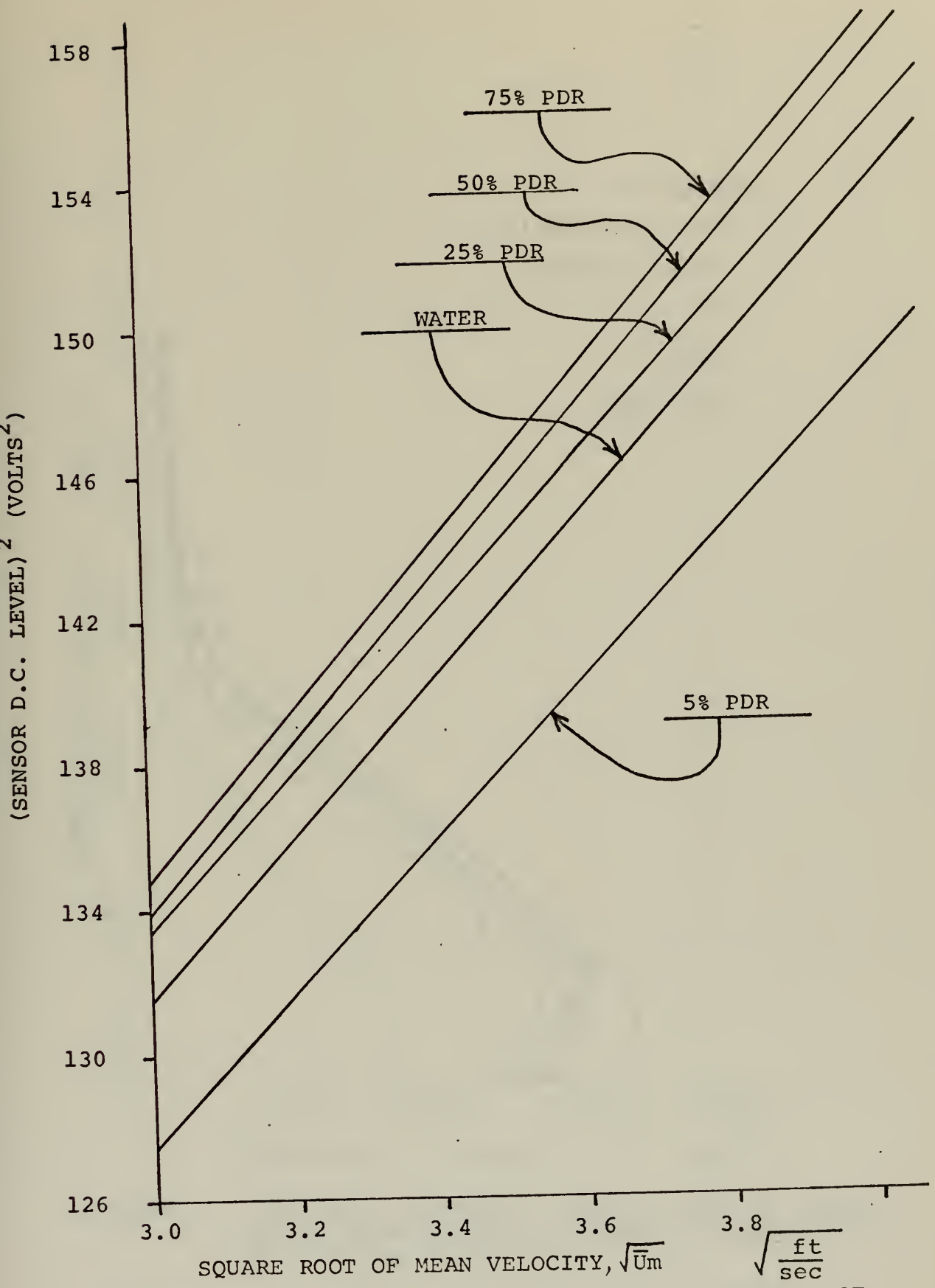

FIGURE 6: TSI HOT-FILM CALIBRATION AS A FUNCTION OF POLYMER SOLUTION DEGRADATION

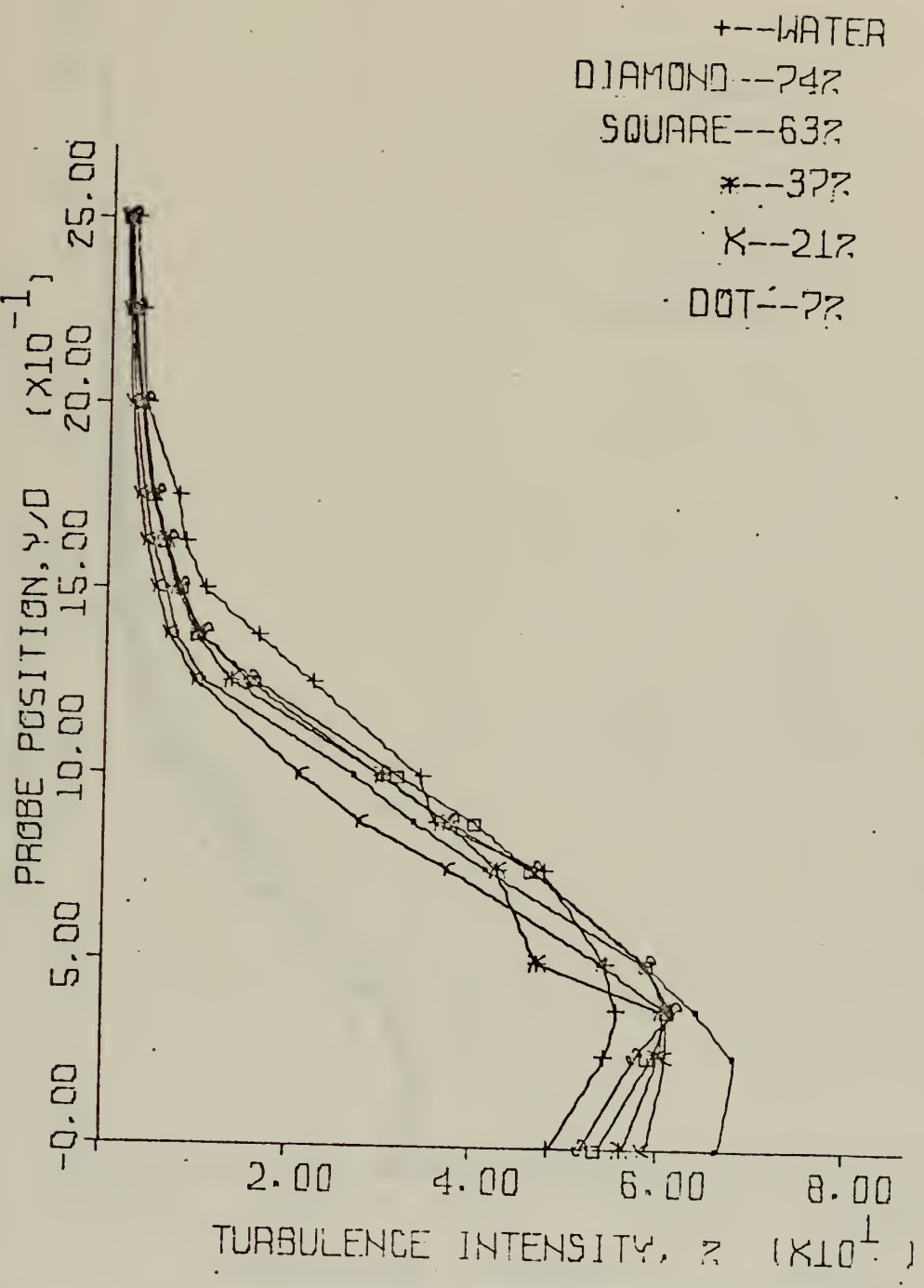

FIGURE 7: TURBULENCE INTENSITY PROFILES FOR TAP WATER AND 25 WPPM POLYMER SOLUTIONS, VARIOUS PDR'S; RE = 80,000; X/D = 2.5

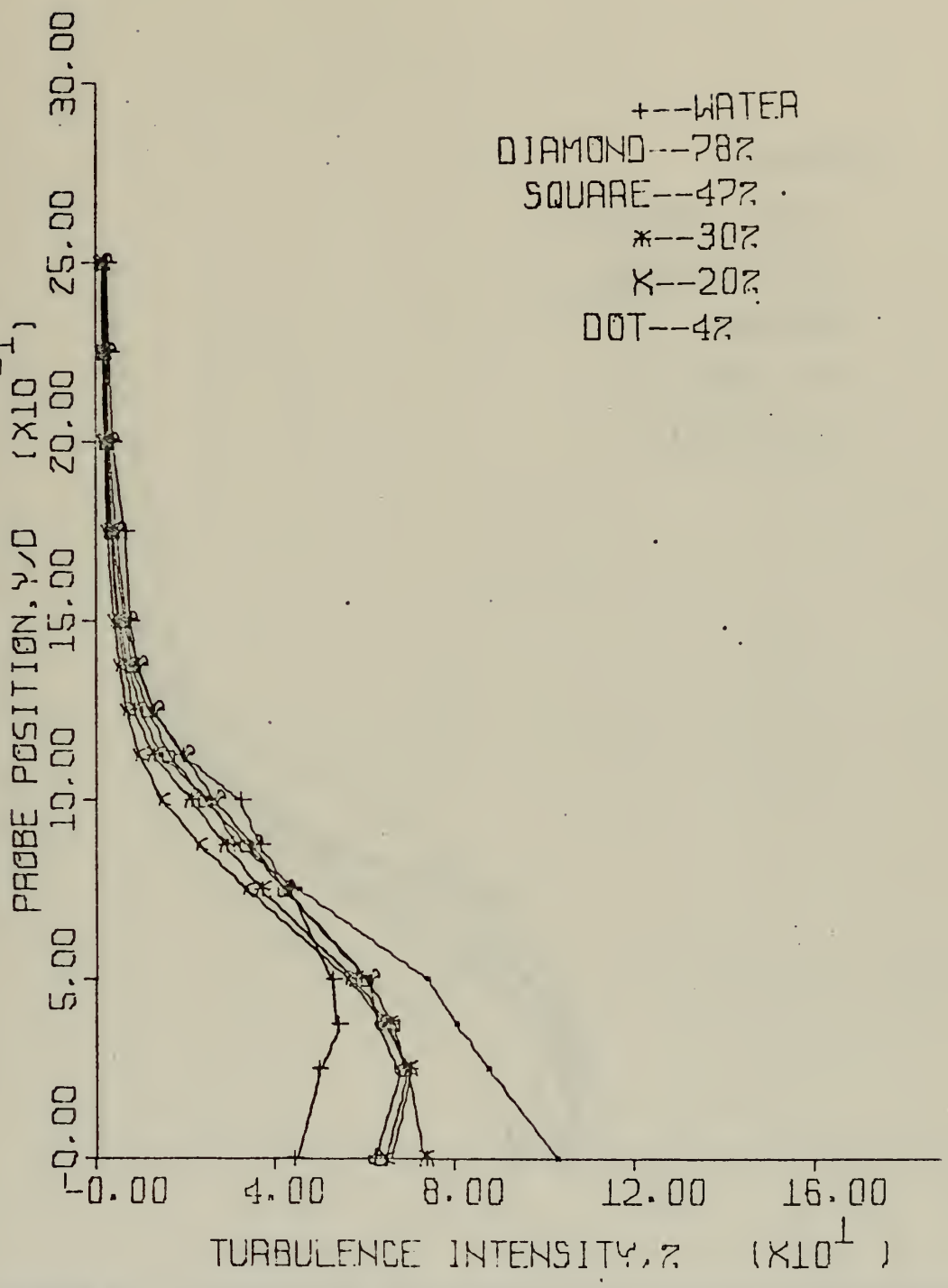

FIGURE 8: TURBULENCE INTENSITY PROFILES FOR TAP WATER AND 25 WPPM POLYMER SOLUTIONS, VARIOUS PDR'S; RE = 100,000; X/D = 2.5

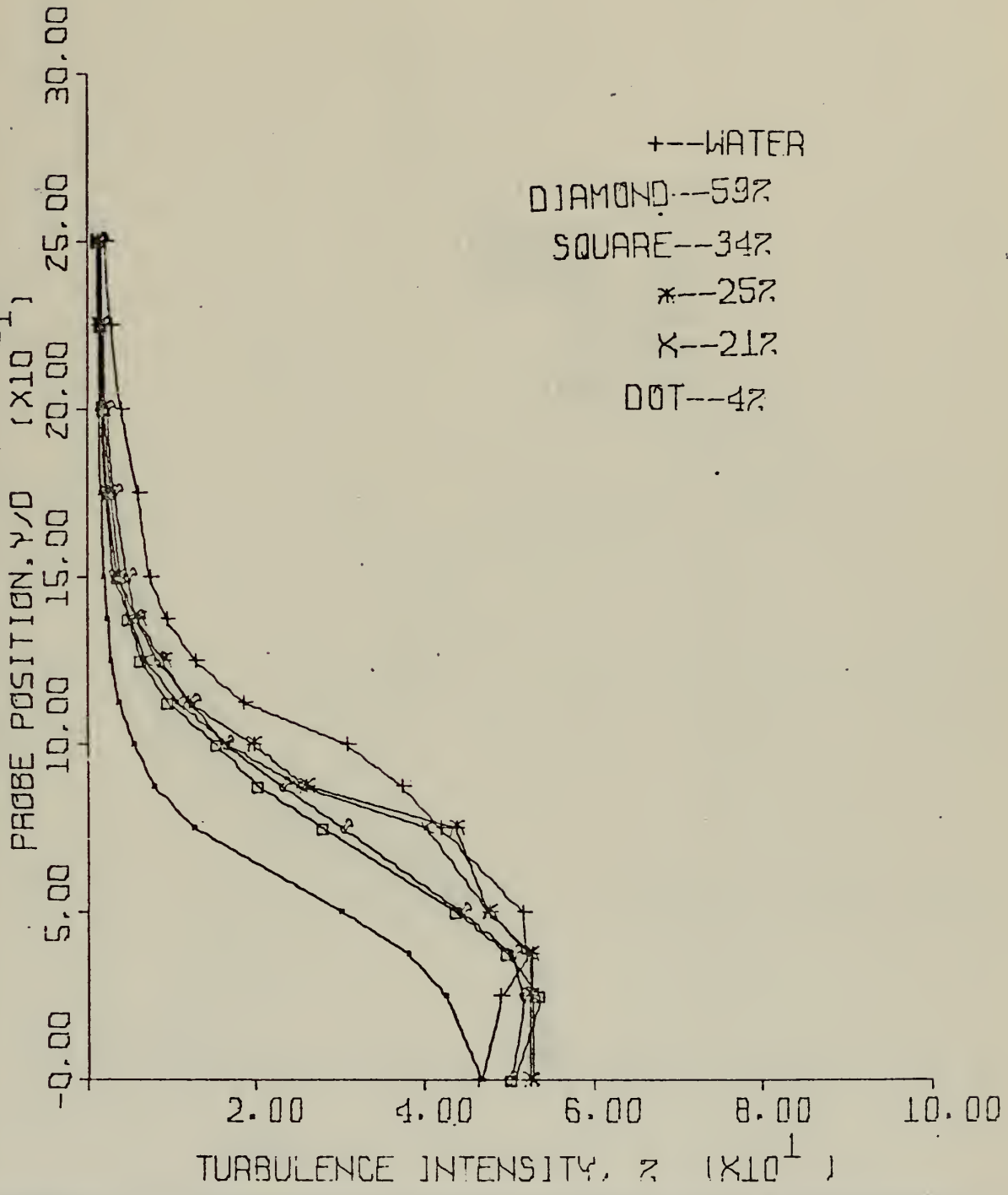

FIGURE 9: TURBULENCE INTENSITY PROFILES FOR TAP WATER AND 25 WPPM POLYMER SOLUTIONS, VARIOUS PDR'S; RE = 120,000; X/D = 2.5

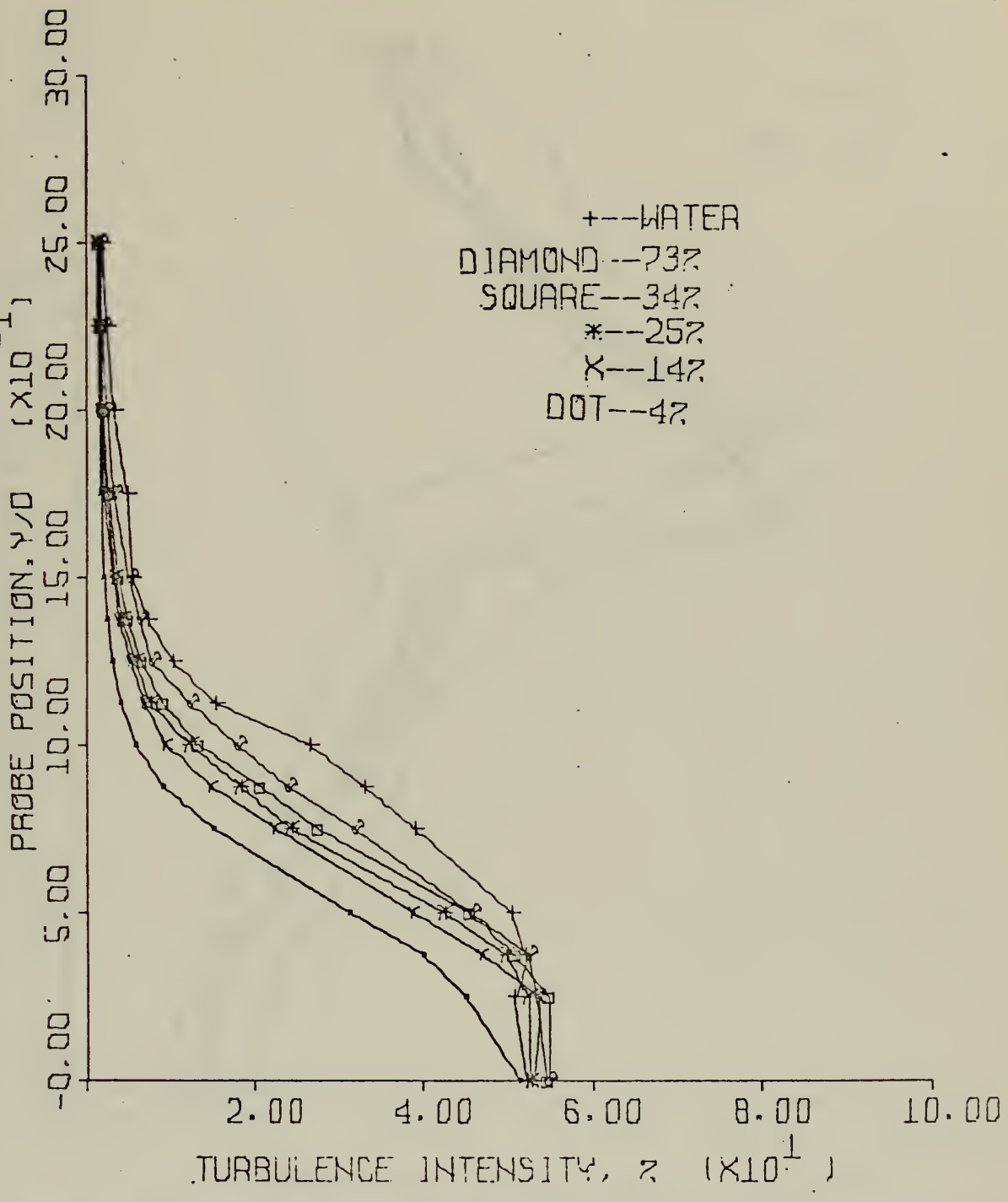

FIGURE 10: TURBULENCE INTENSITY PROFILES FOR TAP WATER AND 25 WPPM POLYMER SOLUTIONS, VARIOUS PDR'S; RE = 140,000; X/D = 2.5

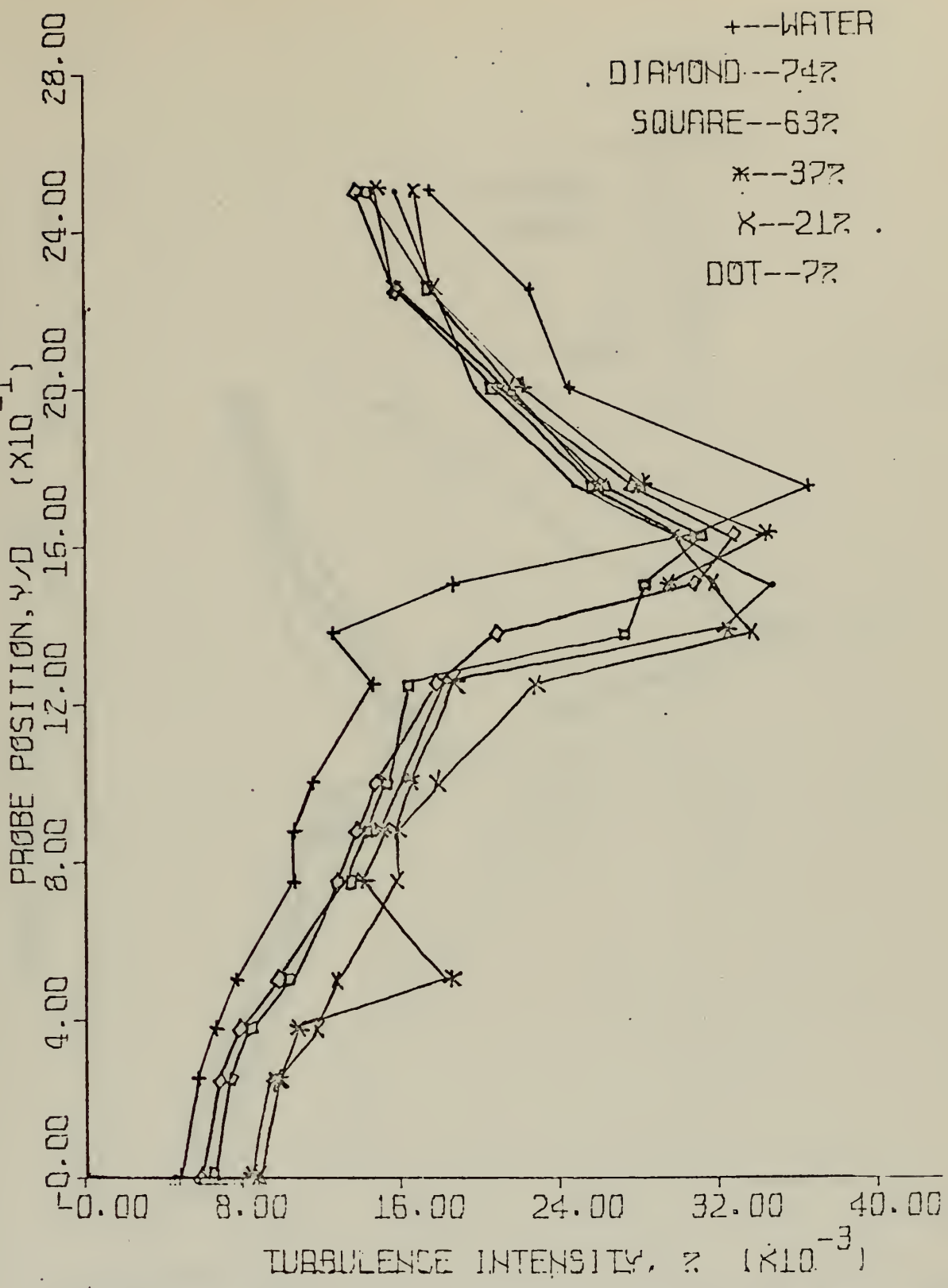

FIGURE 11: MICROSCALE OF TURBULENCE PROFILES FOR TAP WATER AND 25 WPPM POLYMER SOLUTIONS; VARIOUS PDR'S; RE = 80,000; X/D = 2.5

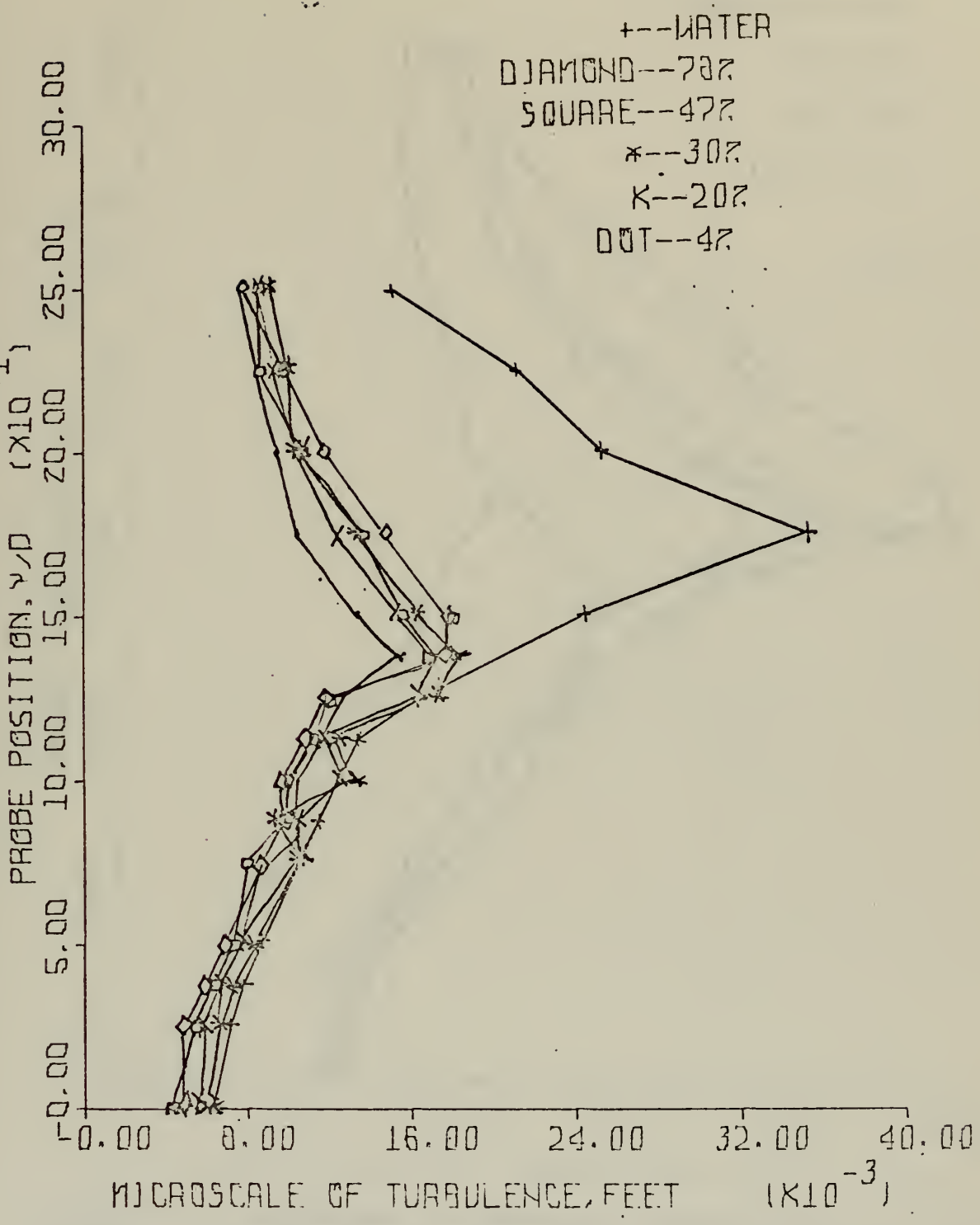

FIGURE 12: MICROSCALE OF TURBULENCE PROFILES FOR TAP WATER AND 25 WPPM POLYMER SOLUTIONS; VARIOUS PDR'S; RE = 100,000; X/D = 2.5

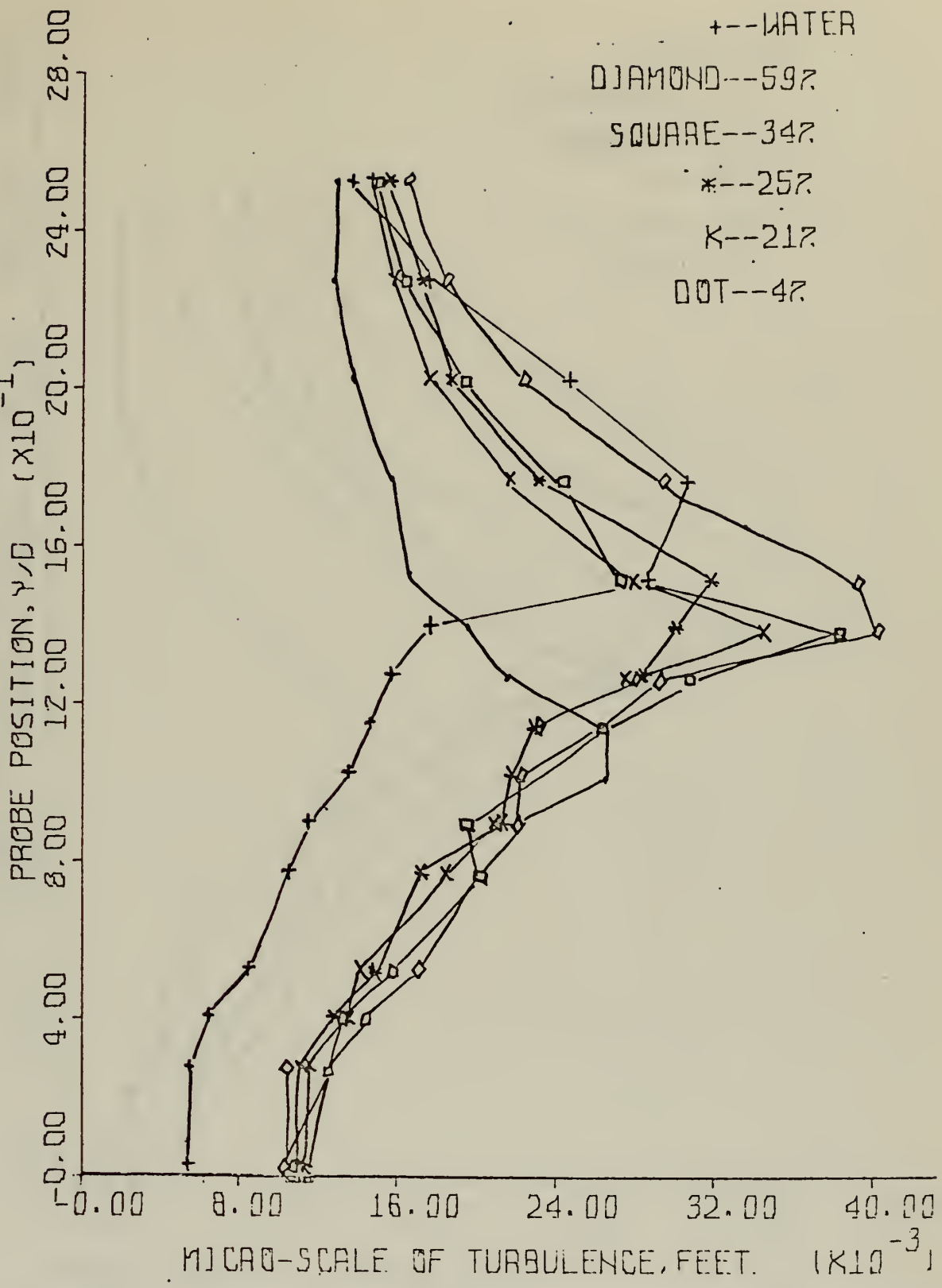

FIGURE 13: MICROSCALE OF TURBULENCE PROFILES FOR TAP WATER AND 25 WPPM POLYMER SOLUTIONS; VARIOUS PDR'S; RE = 120,000; X/D = 2.5

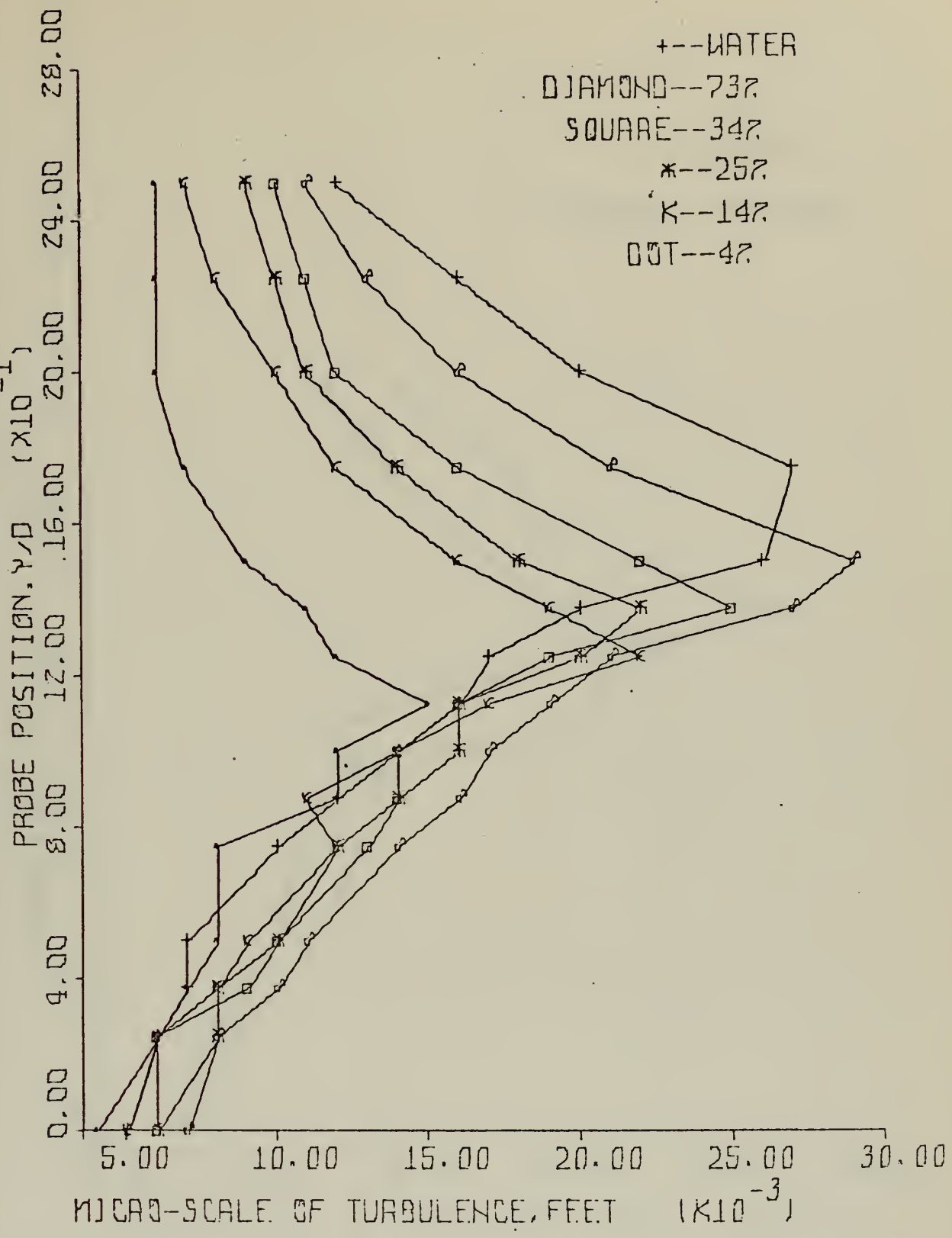

FIGURE 14: MICROSCALE OF TURBULENCE PROFILES FOR TAP WATER AND 25 WPPM POLYMER SOLUTION; VARIOUS PDR'S; RE = 140,000; X/D = 2.5

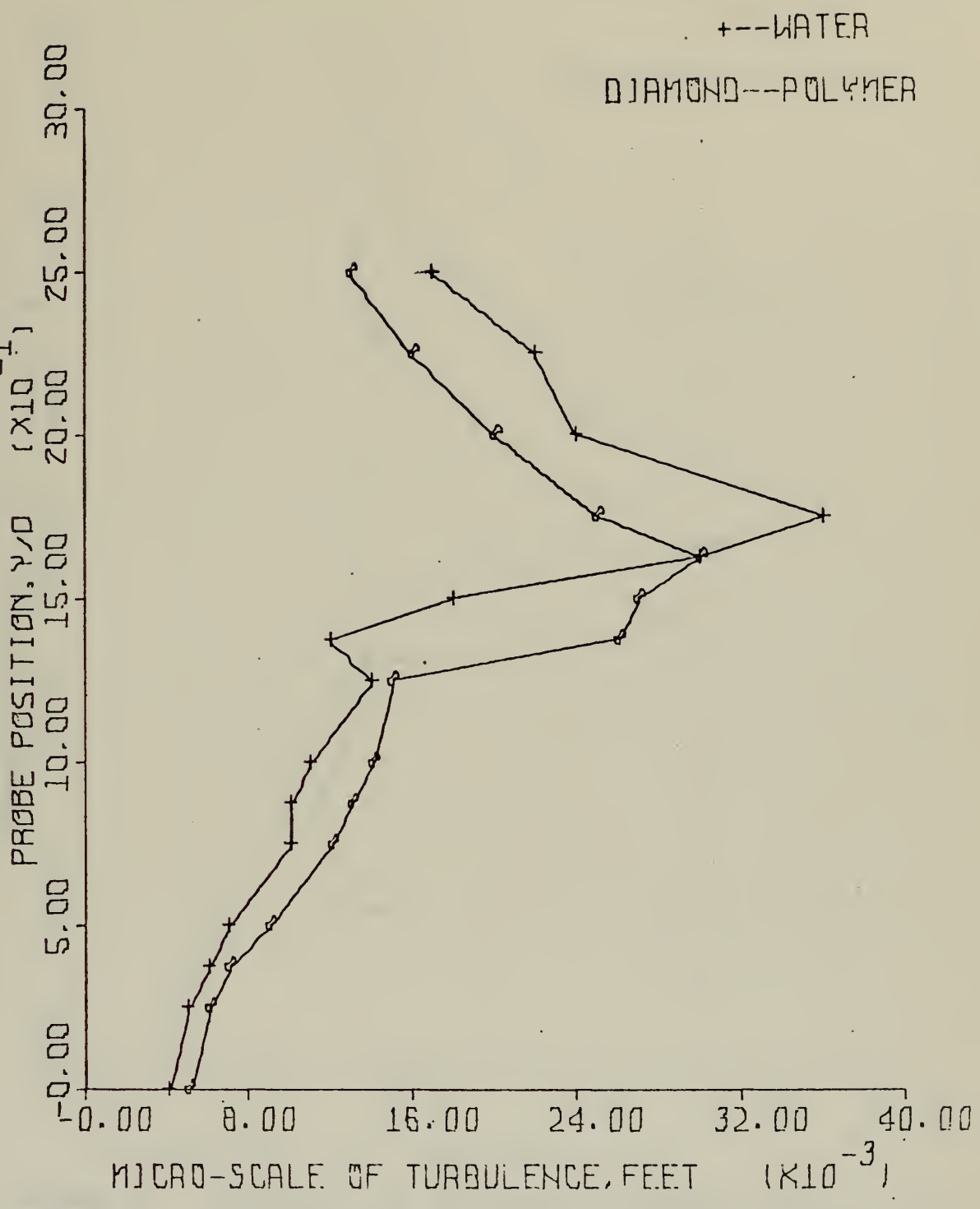

FIGURE 15: MICROSCALE OF TURBULENCE PROFILES FOR TAP WATER AND 25 WPPM POLYMER SOLUTION; 63% PDR; RE = 80,000; X/D = 2.5

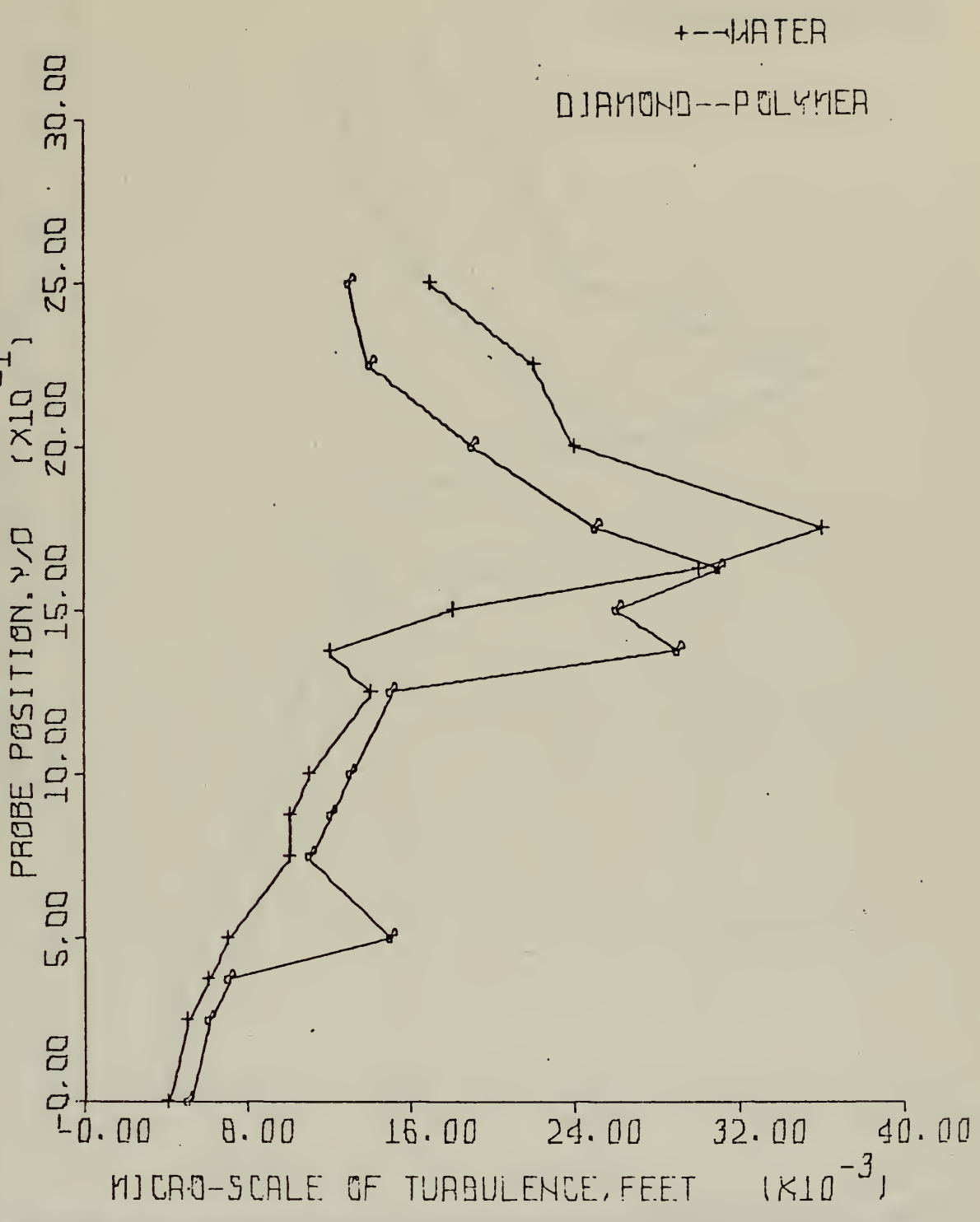

FIGURE 16: MICROSCALE OF TURBULENCE PROFILES FOR TAP WATER AND 25 WPPM POLYMER SOLUTION; 37% PDR; RE = 80,000; X/D = 2.5

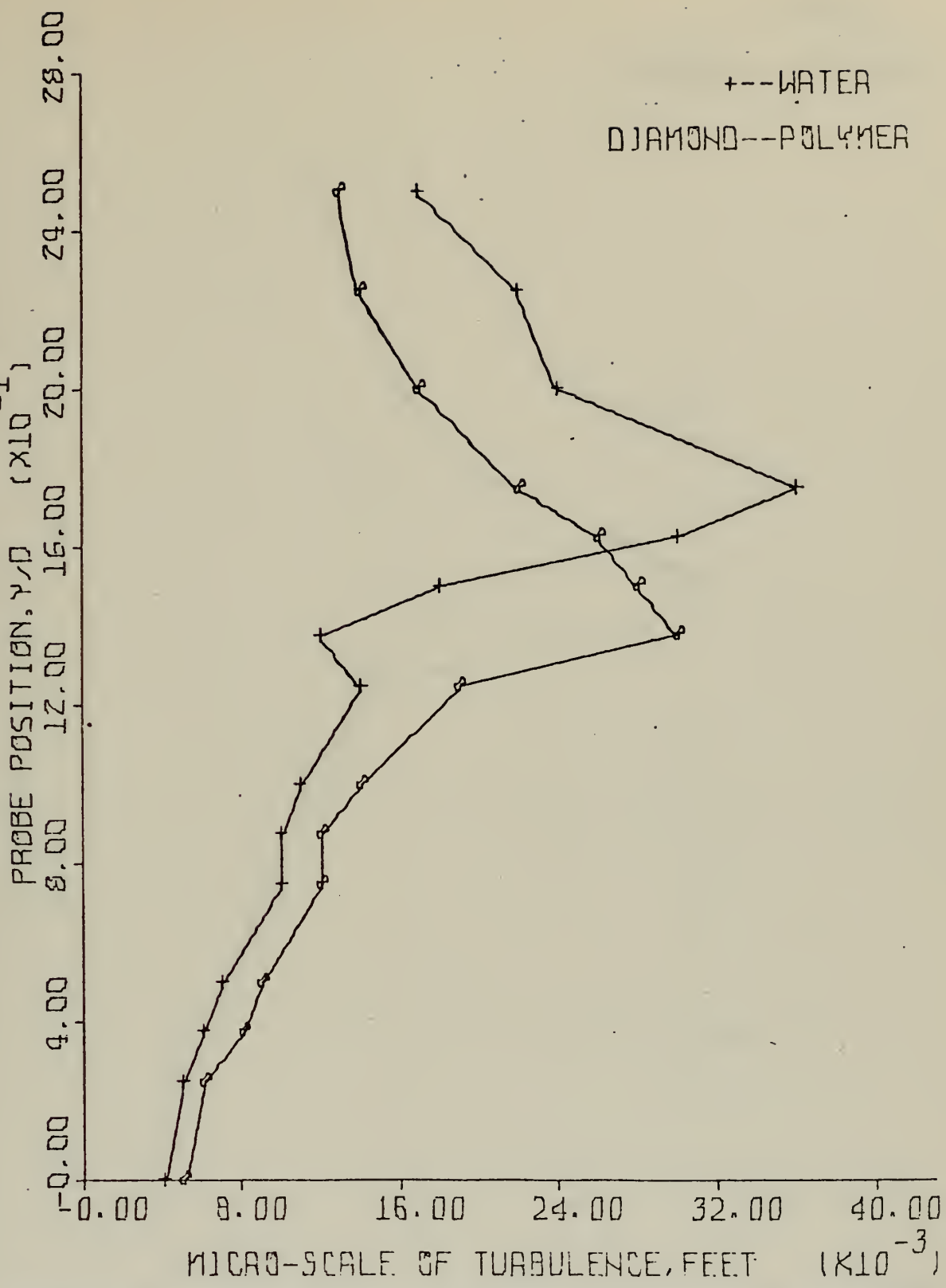

FIGURE 17: MICROSCALE OF TURBULENCE PROFILES FOR TAP WATER AND 25 WPPM POLYMER SOLUTION; 21% PDR; RE = 80,000; X/D = 2.5

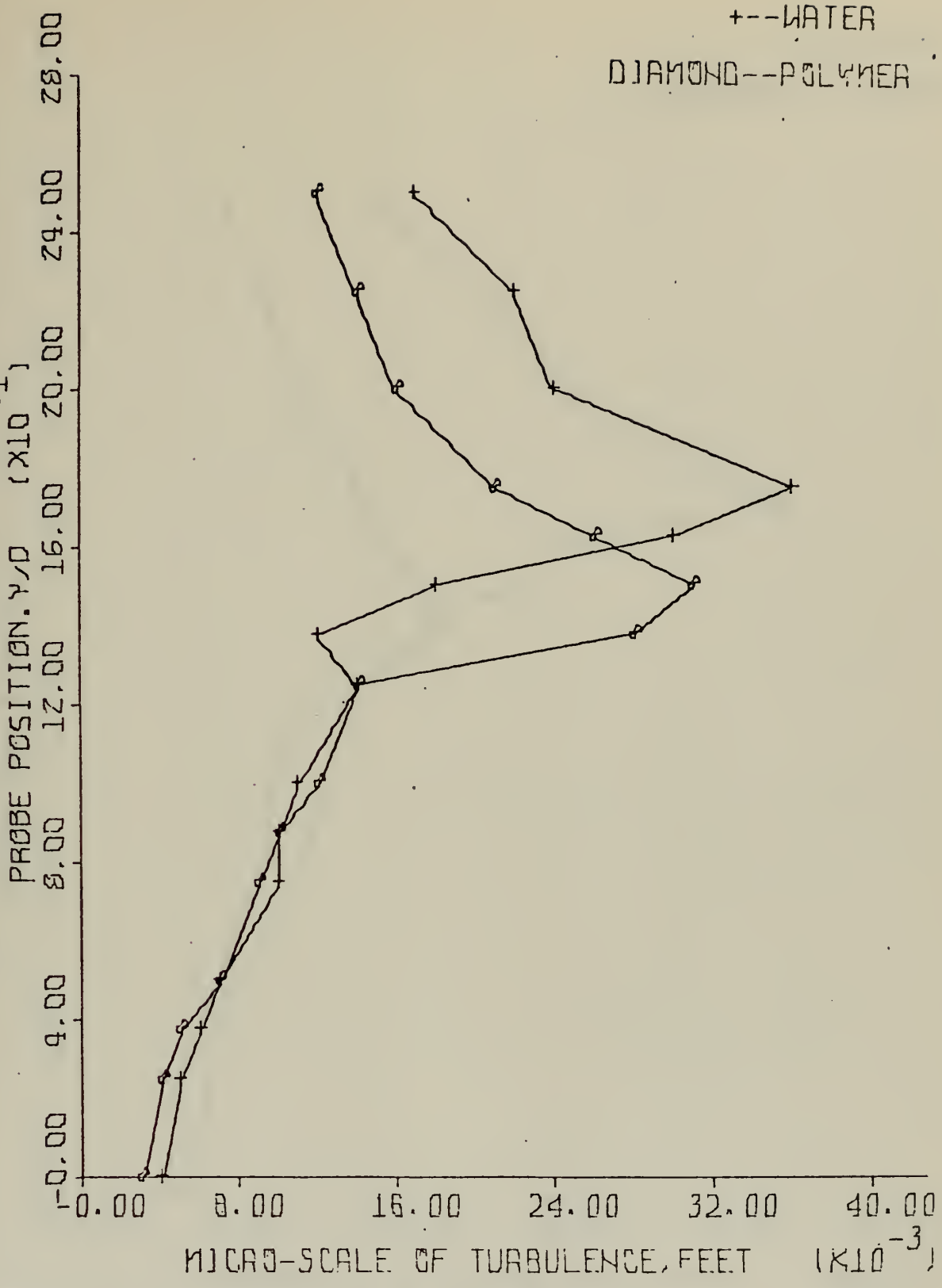

FIGURE 18: MICROSCALE OF TURBULENCE PROFILES FOR TAP WATER AND 25 WPPM POLYMER SOLUTIONS; 7% PDR; RE = 80,000; X/D = 2.5

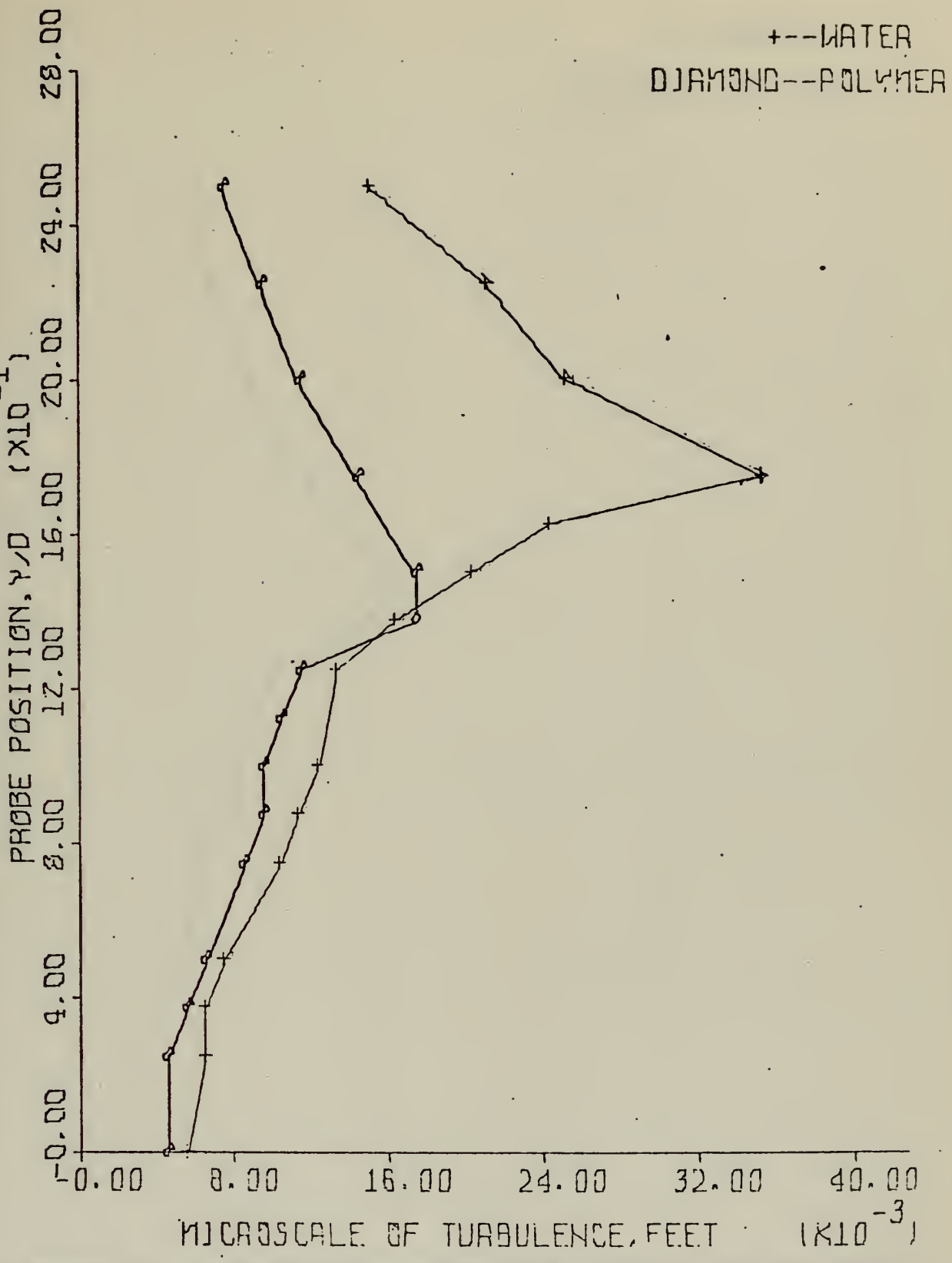

FIGURE 19: MICROSCALE OF TURBULENCE PROFILES FOR TAP WATER AND 25 WPPM POLYMER SOLUTIONS; 78% PDR; RE = 100,000; X/D = 2.5

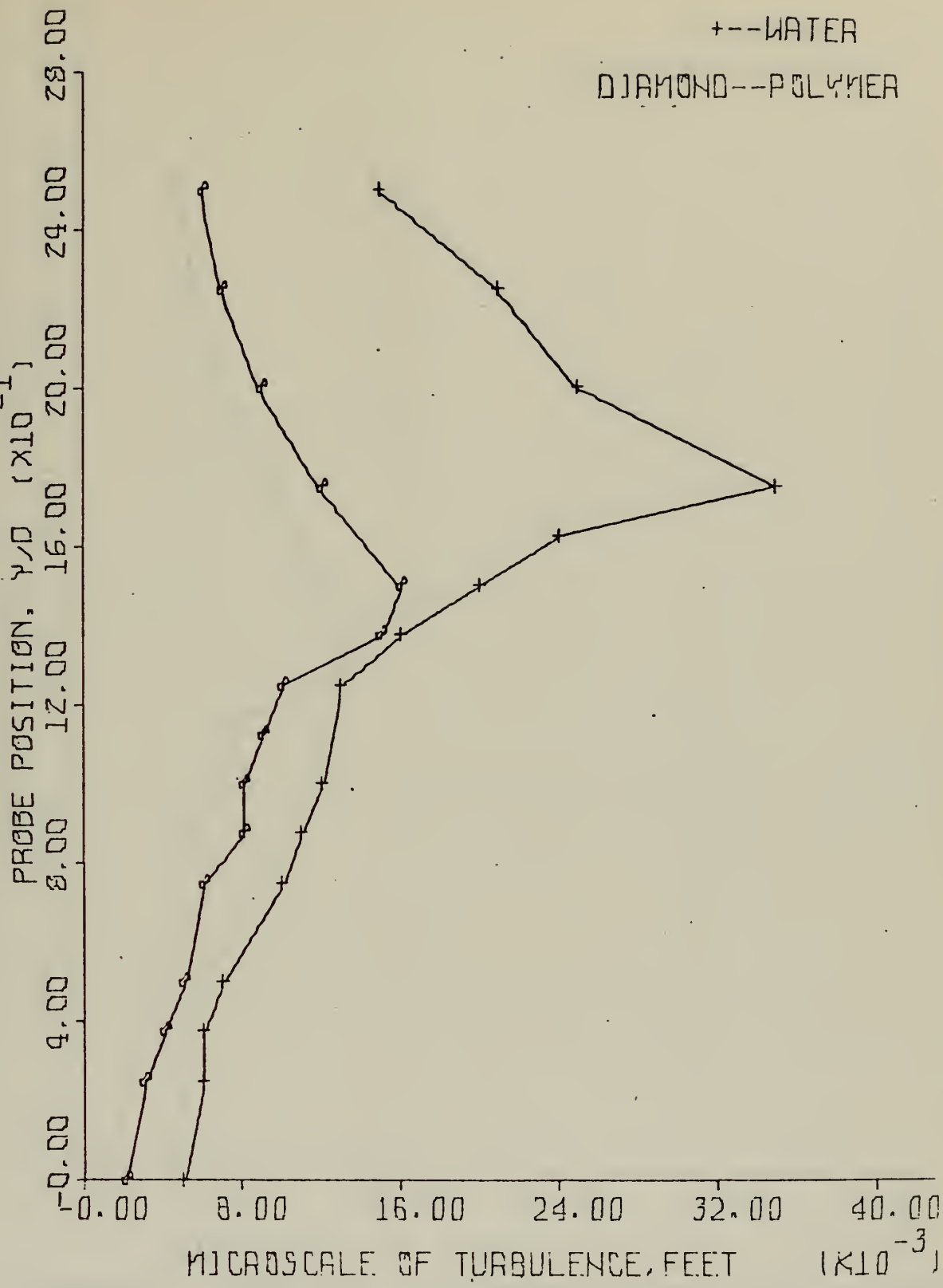

FIGURE 20: MICROSCALE OF TURBULENCE PROFILES FOR TAP WATER AND 25 WPPM POLYMER SOLUTIONS; 47% PDR; RE = 100,000; X/D = 2.5

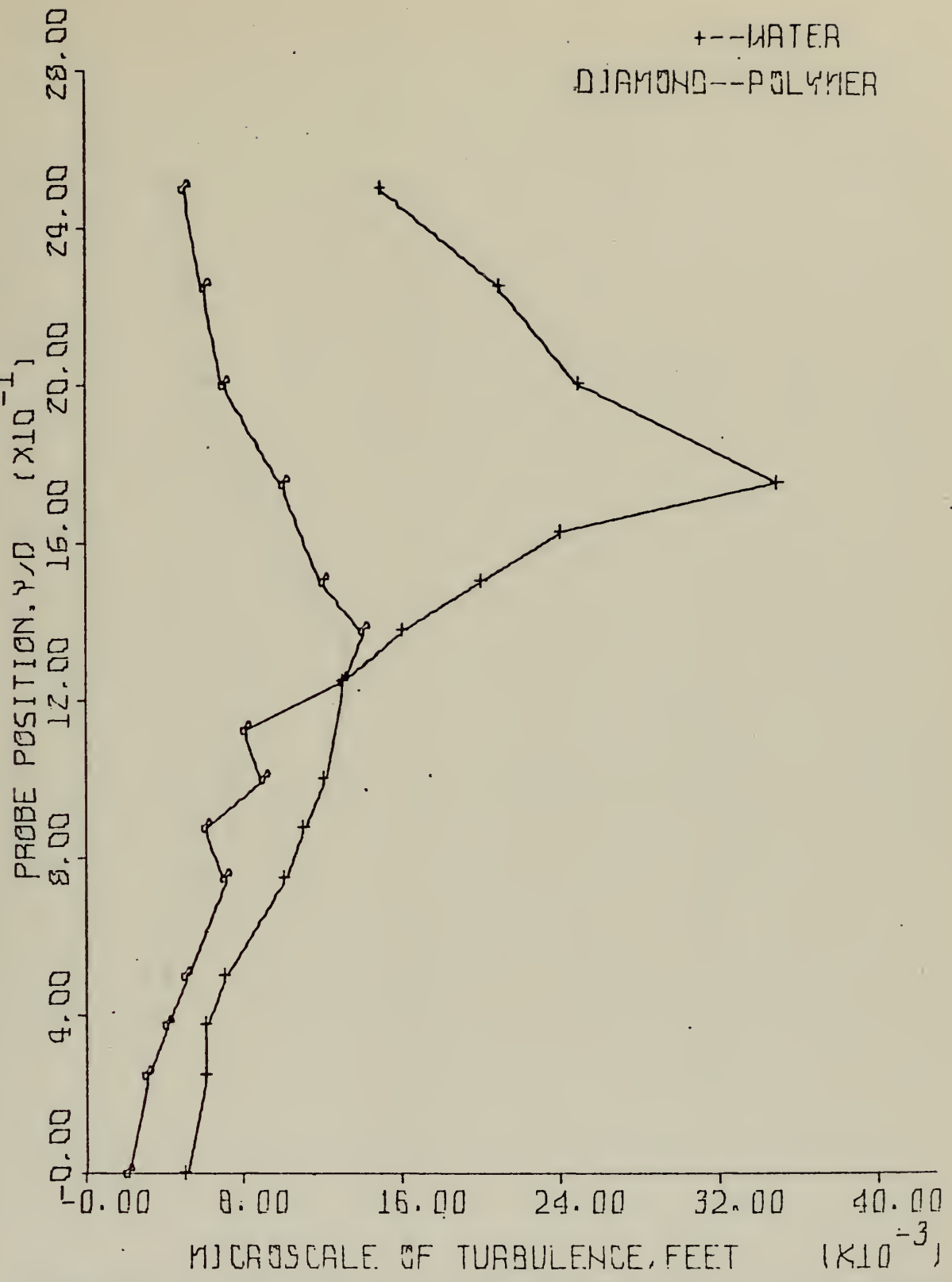

FIGURE 21: MICROSCALE OF TURBULENCE PROFILES FOR TAP WATER AND 25 WPPM POLYMER SOLUTIONS; 30% PDR; RE = 100,000; X/D = 2.5

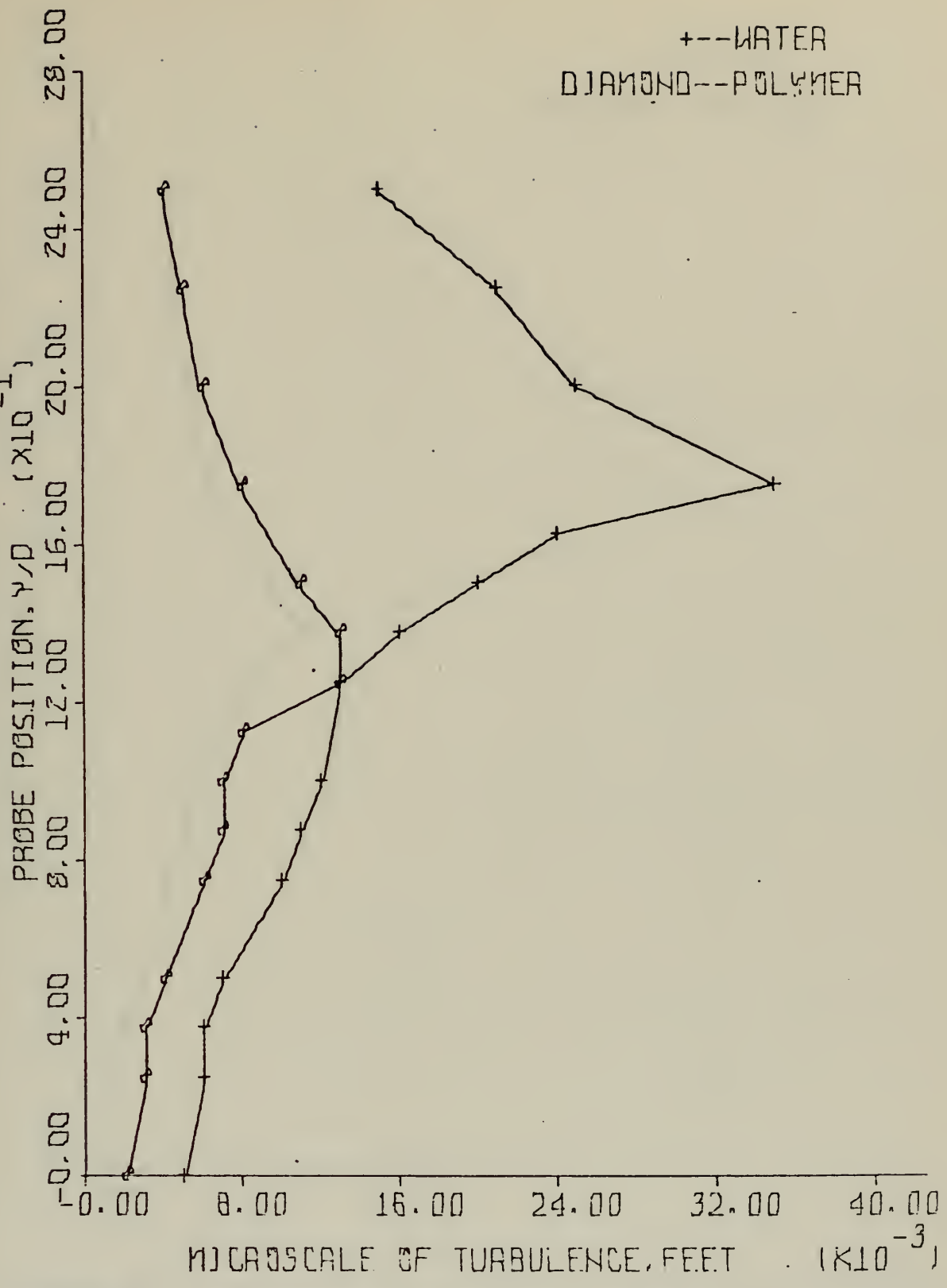

FIGURE 22: MICROSCALE OF TURBULENCE PROFILES FOR TAP WATER AND 25 WPPM POLYMER SOLUTIONS; 20% PDR; RE = 100,000; X/D = 2.5

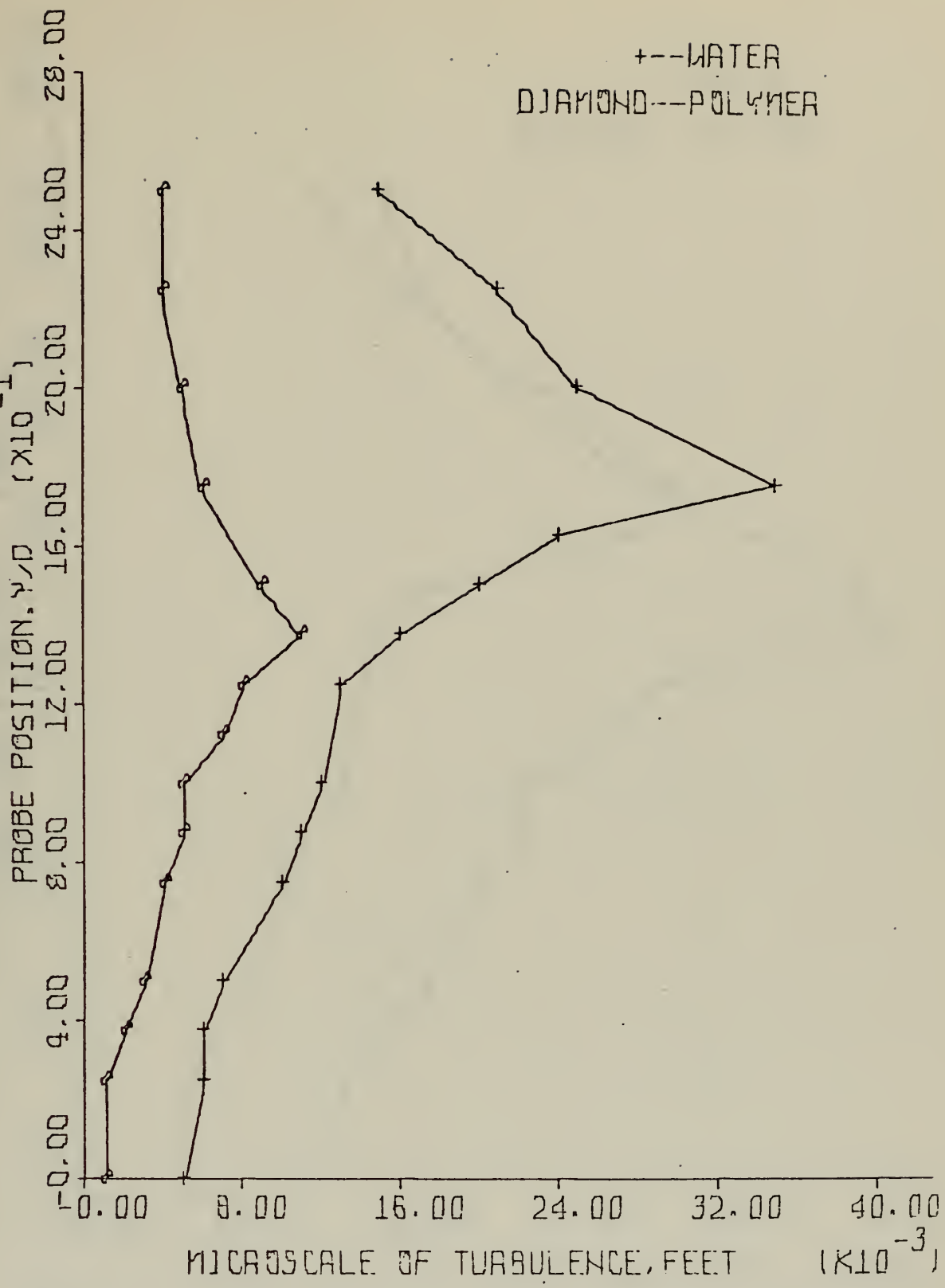

FIGURE 23: MICROSCALE OF TURBULENCE PROFILES FOR TAP WATER AND 25 WPPM POLYMER SOLUTIONS; 4% PDR; RE = 100,000; X/D = 2.5

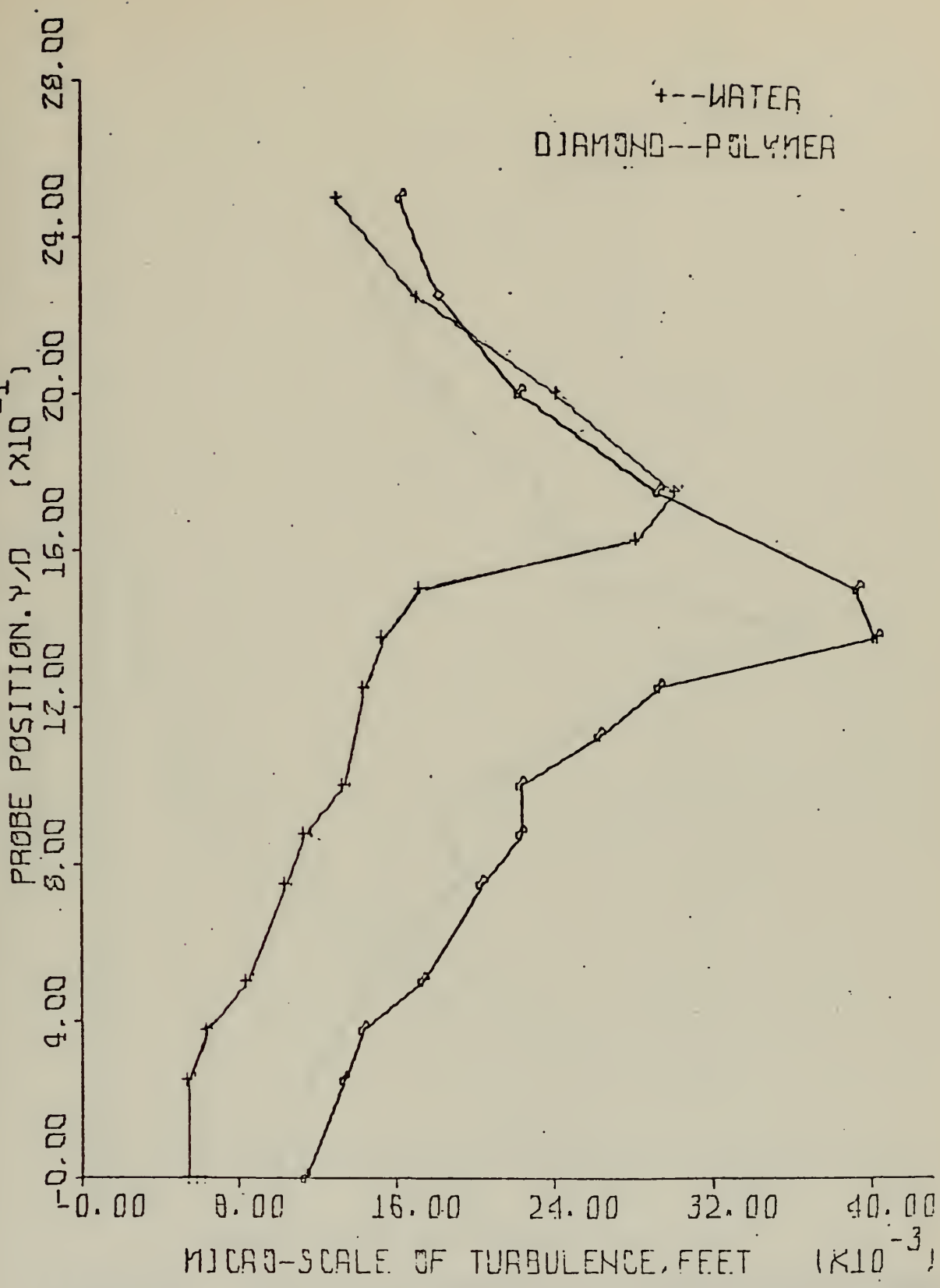

FIGURE 24: MICROSCALE OF TURBULENCE PROFILES FOR TAP WATER AND 25 WPPM POLYMER SOLUTIONS; 59% PDR; RE = 120,000; X/D = 2.5

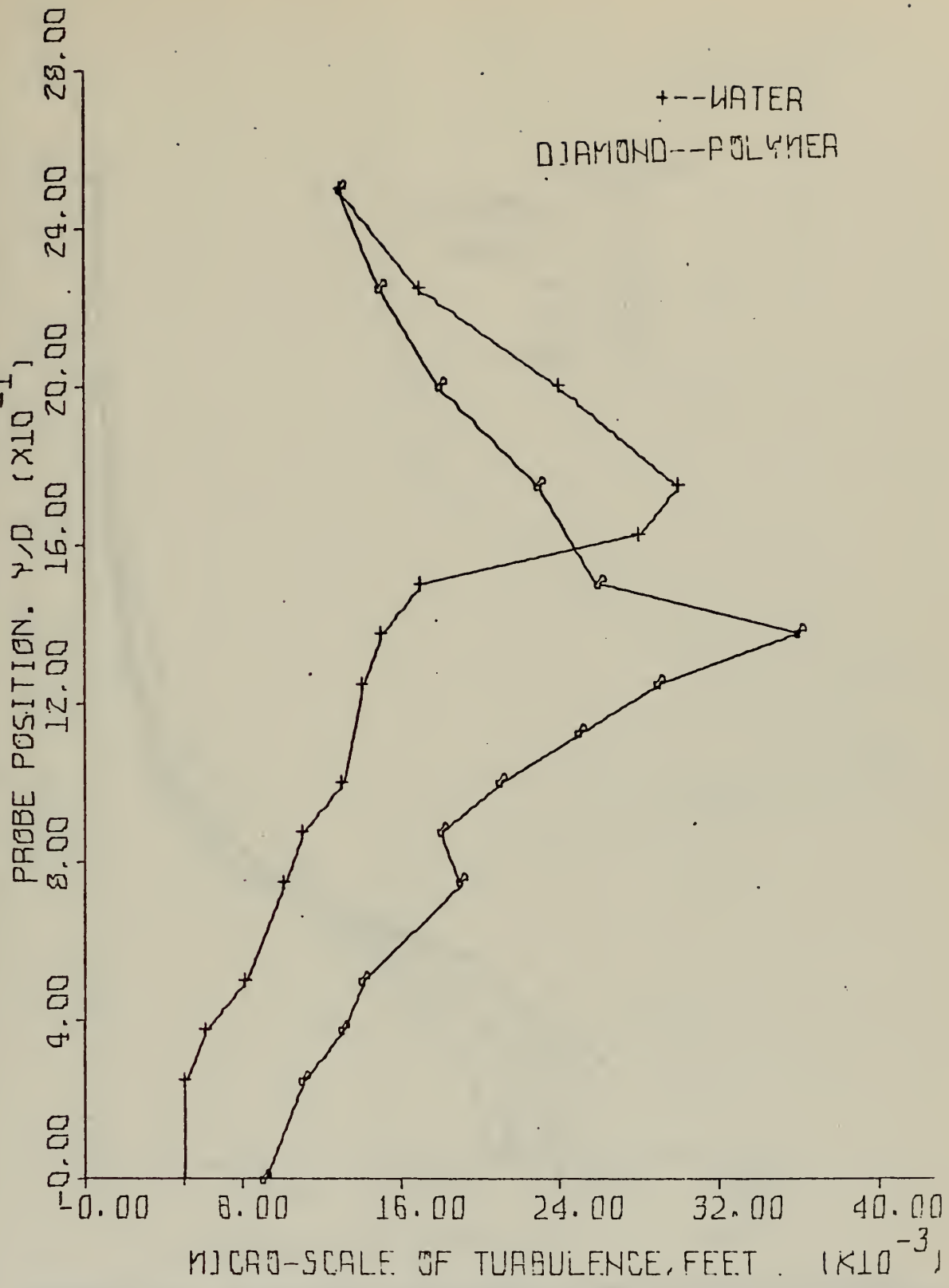

FIGURE 25: MICROSCALE OF TURBULENCE PROFILES FOR TAP WATER AND 25 WPPM POLYMER SOLUTIONS; 34% PDR; RE = 120,000; X/D = 2.5

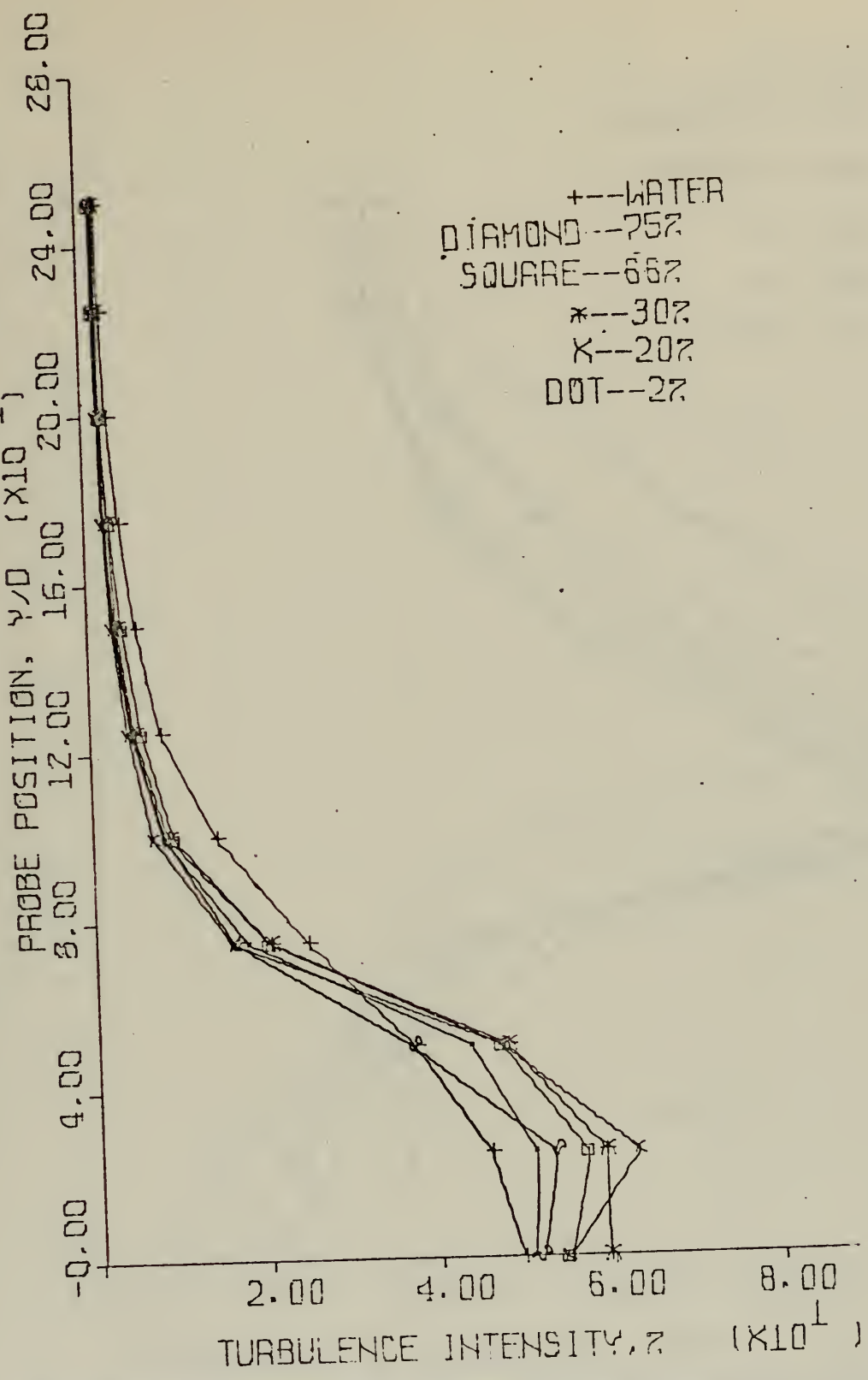

FIGURE 26: TURBULENCE INTENSITY PROFILES FOR TAP WATER AND 25 WPPM POLYMER SOLUTIONS; VARIOUS PDR'S; RE = 80,000; X/D = 1.5

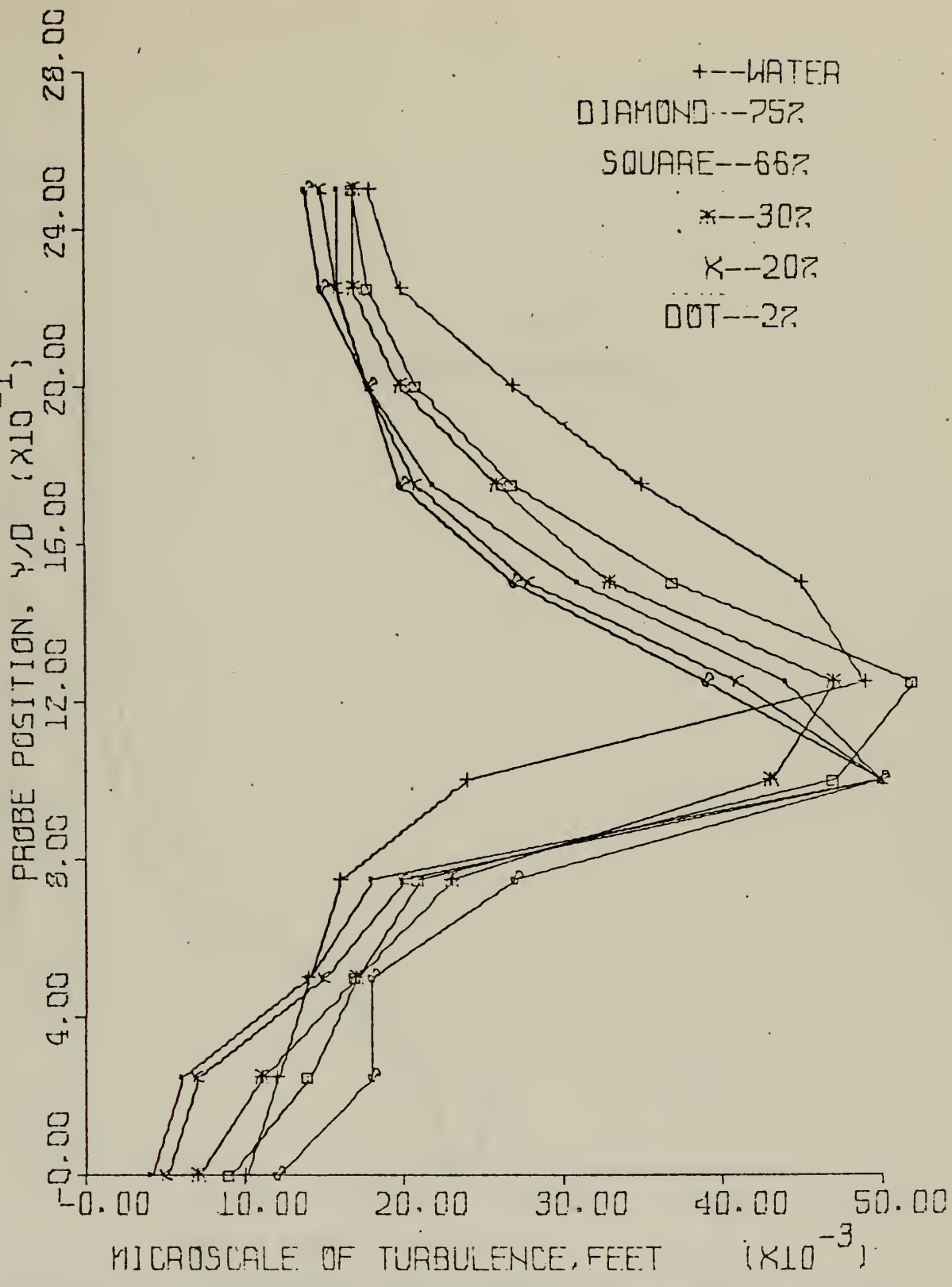

FIGURE 27: MICROSCALE OF TURBULENCE PROFILES FOR TAP WATER AND 25 WPPM POLYMER SOLUTIONS; VARIOUS PDR'S; RE = 80,000; X/D = 1.5

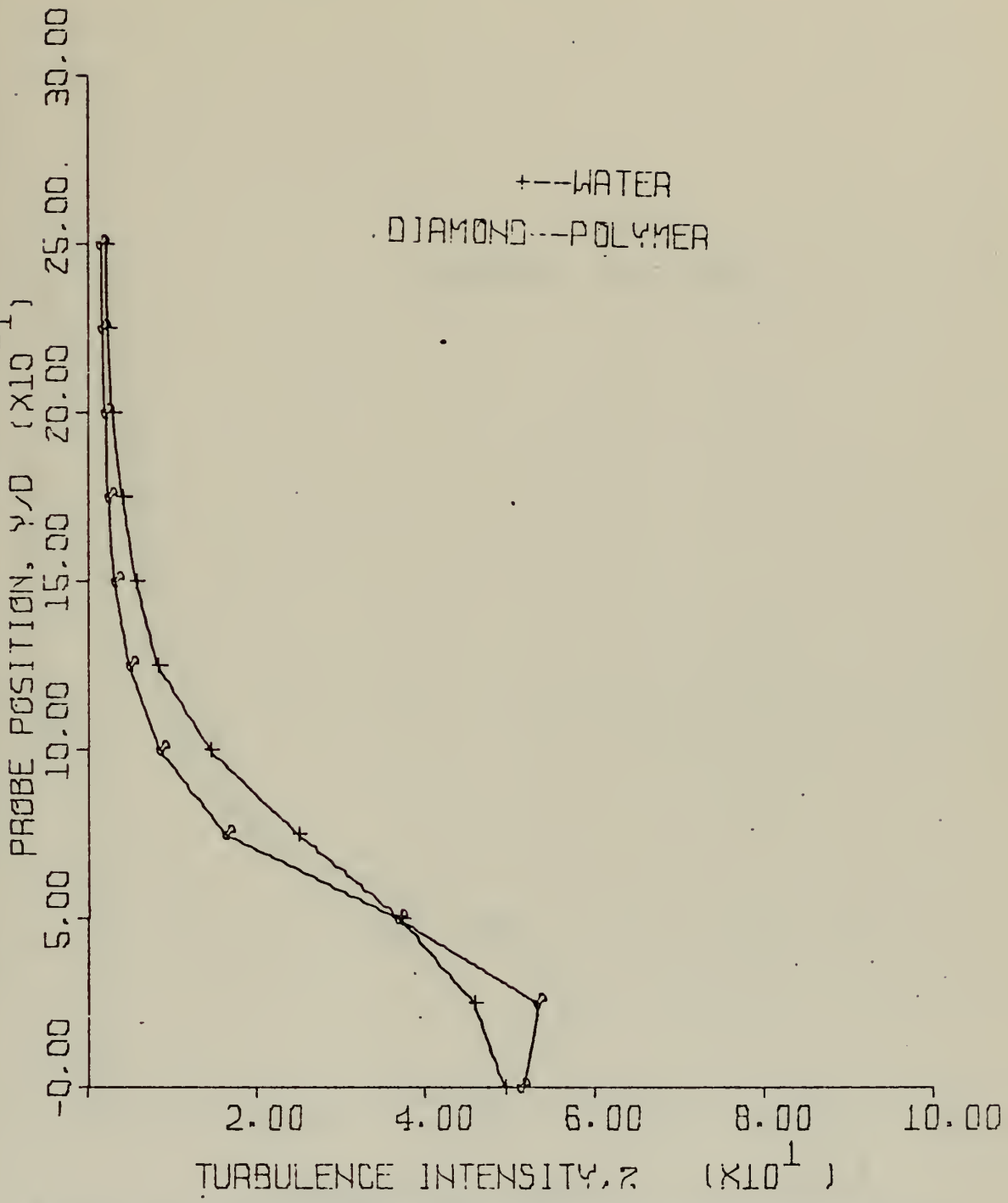

FIGURE 28: TURBULENCE INTENSITY PROFILES FOR TAP WATER AND 25 WPPM POLYMER SOLUTIONS; 75% PDR; RE = 80,000; X/D = 1.5

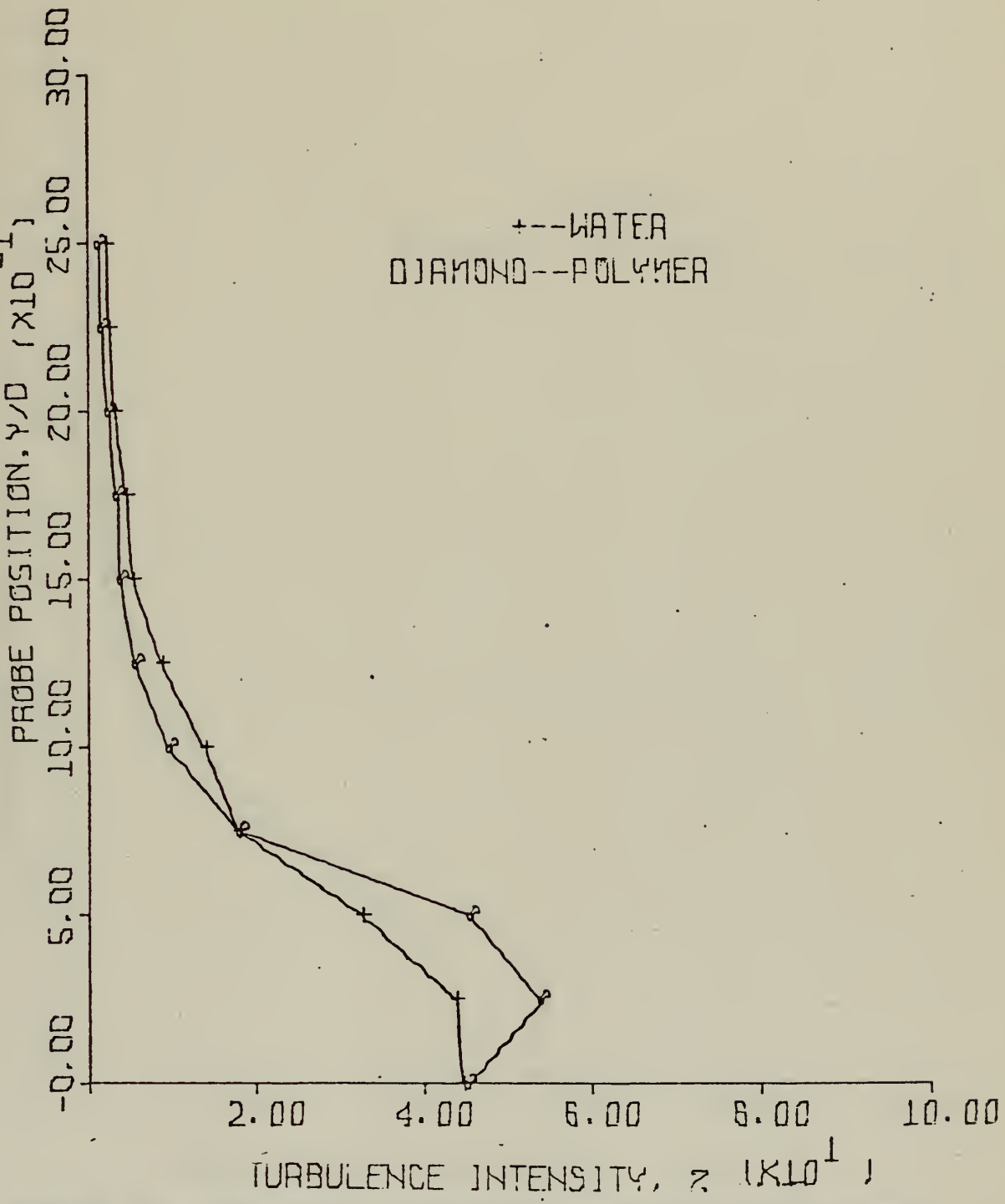

FIGURE 29: SCHIMMELS' TURBULENCE INTENSITY PROFILES FOR TAP WATER AND 25 WPPM POLYMER SOLUTIONS; 70% PDR; RE = 80,000; X/D = 1.5

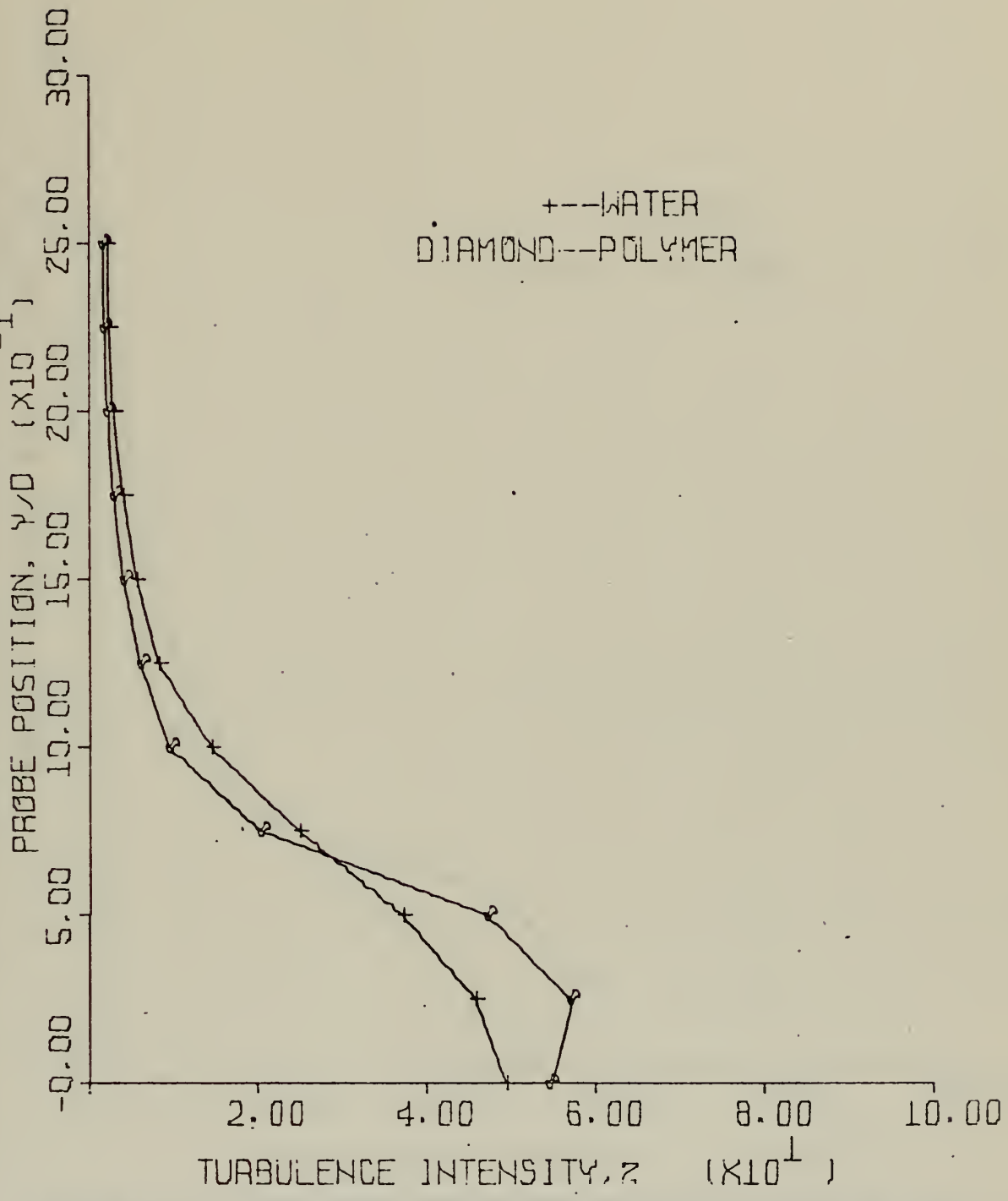

FIGURE 30: TURBULENCE INTENSITY PROFILES FOR TAP WATER AND 25 WPPM POLYMER SOLUTIONS; 66% PDR; RE = 80,000; X/D = 1.5

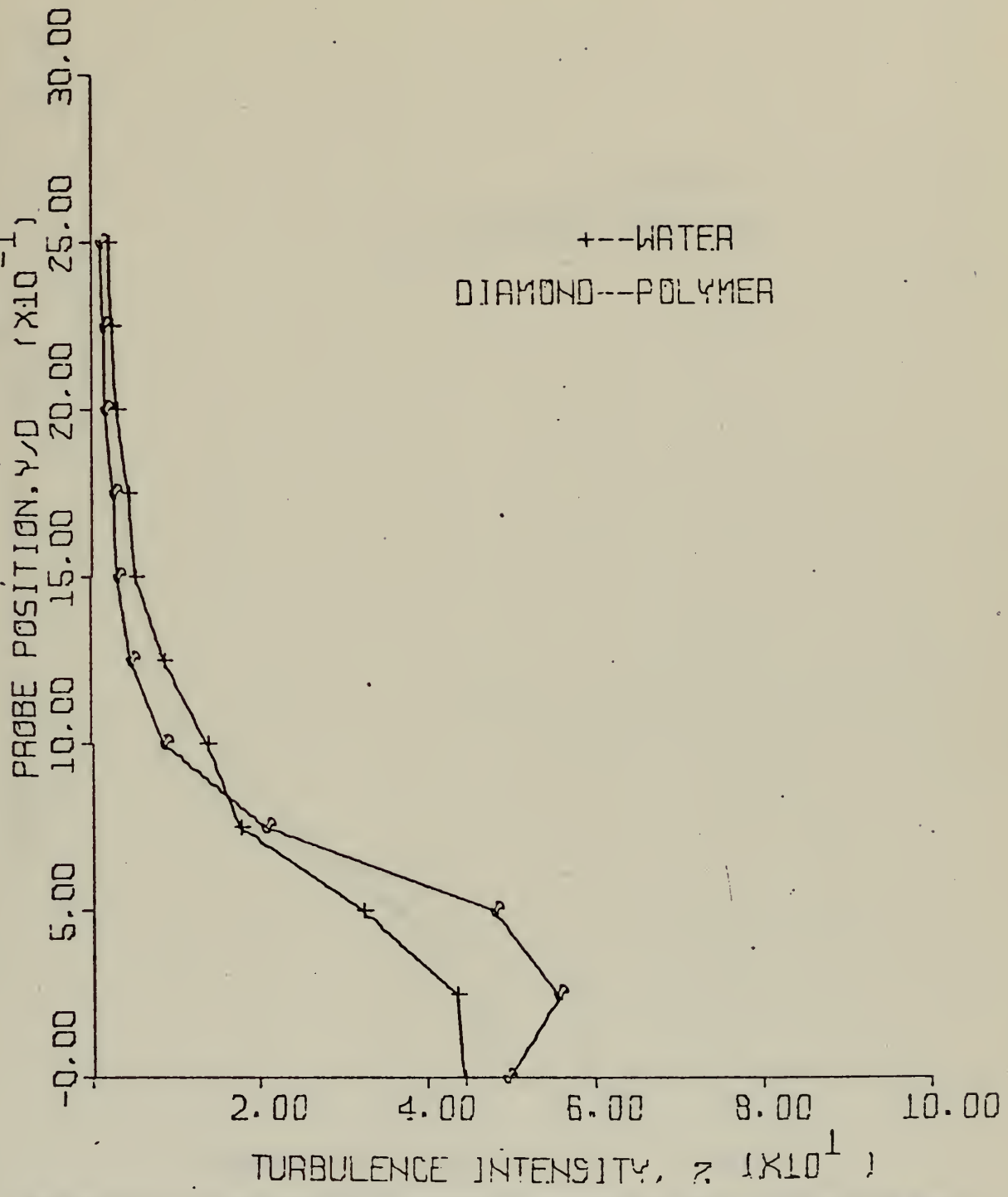

FIGURE 31: SCHIMMELS' TURBULENCE INTENSITY PROFILES FOR TAP WATER AND 25 WPPM POLYMER SOLUTIONS; 57% PDR; RE = 80,000; X/D = 1.5

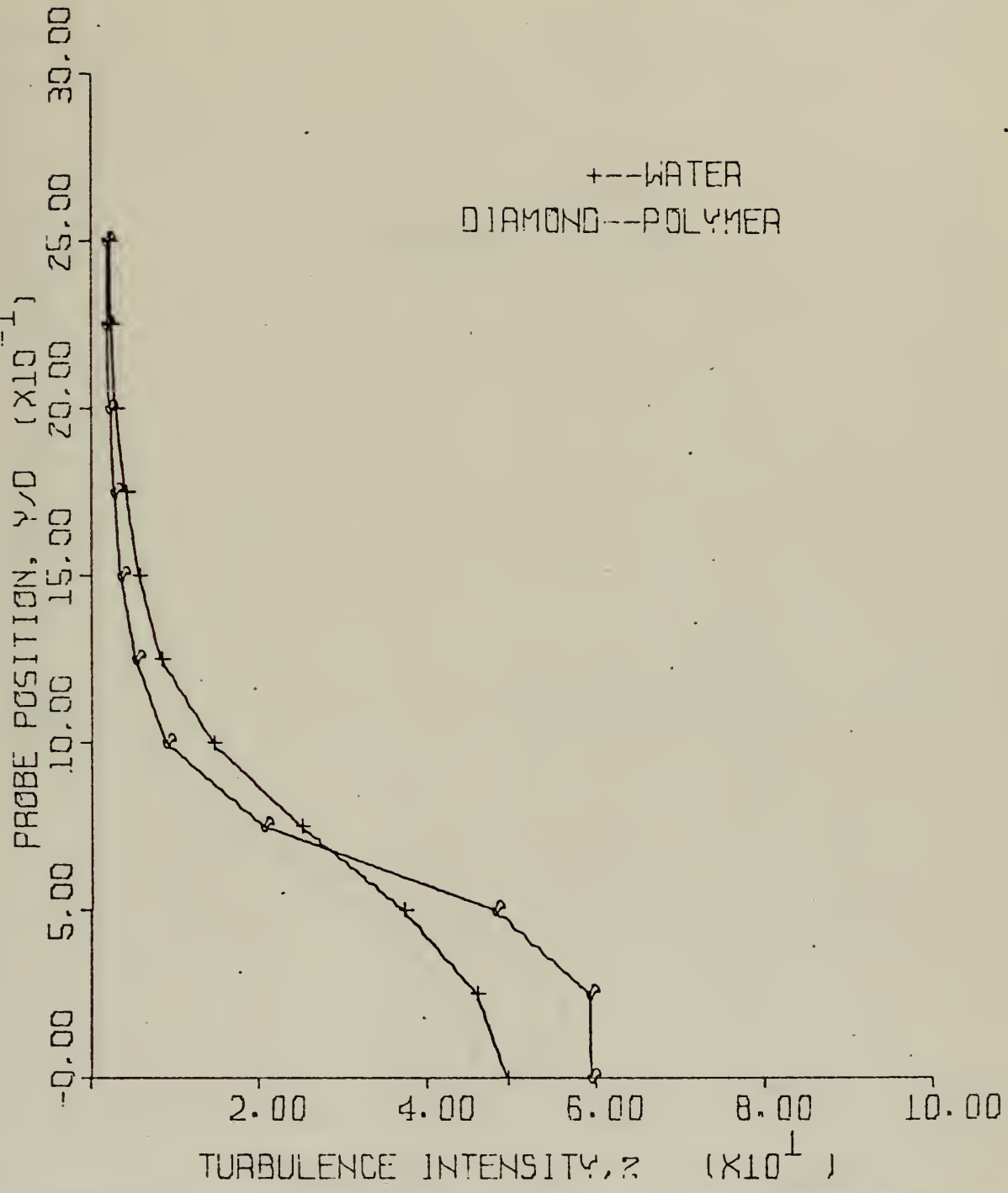

FIGURE 32: TURBULENCE INTENSITY PROFILES FOR TAP WATER AND 25 WPPM POLYMER SOLUTIONS; 40% PDR; RE = 80,000; X/D = 1.5

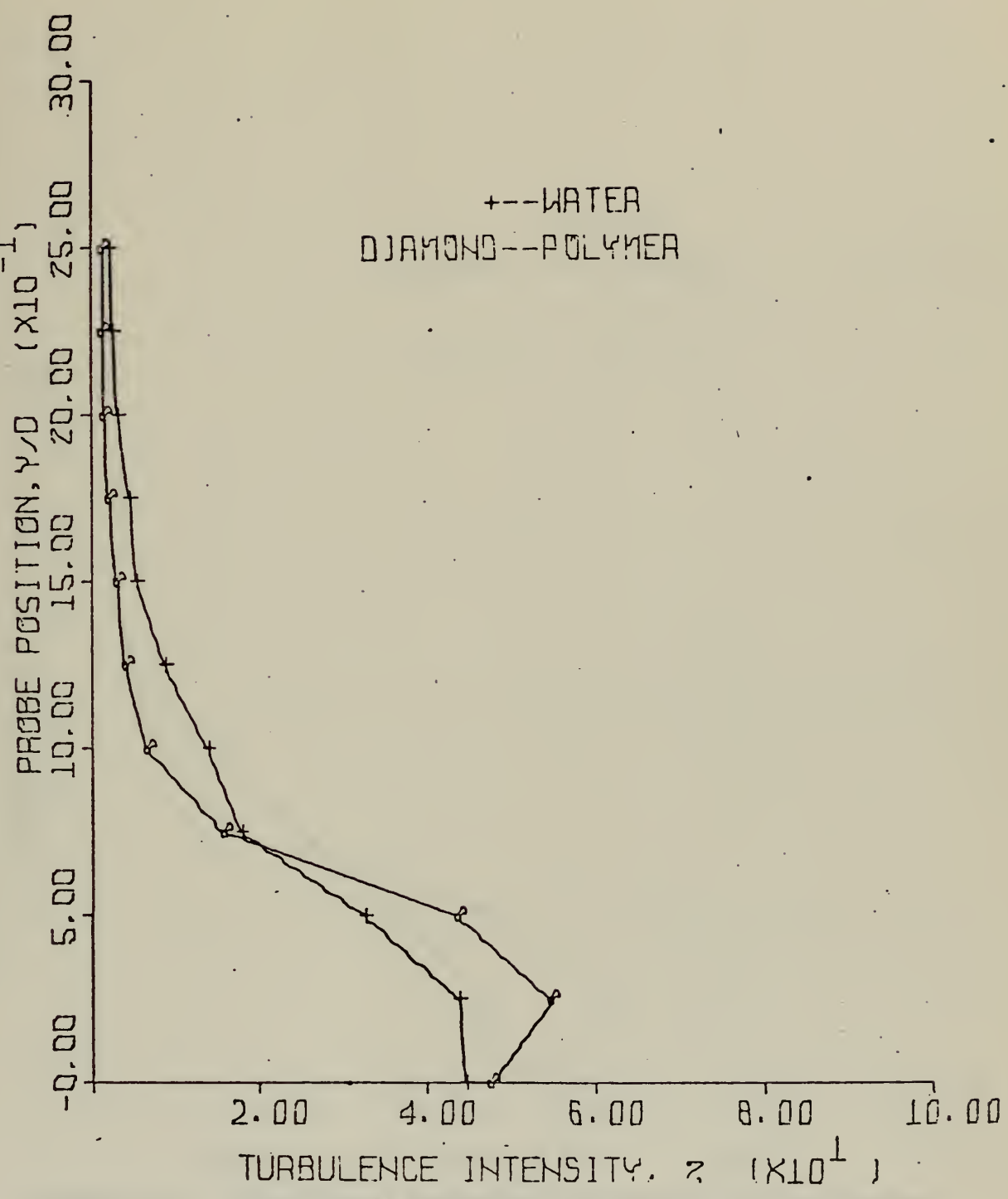

FIGURE 33: SCHIMMELS' TURBULENCE INTENSITY PROFILES FOR TAP WATER AND 25 WPPM POLYMER SOLUTIONS; 38% PDR; RE = 80,000; X/D = 1.5

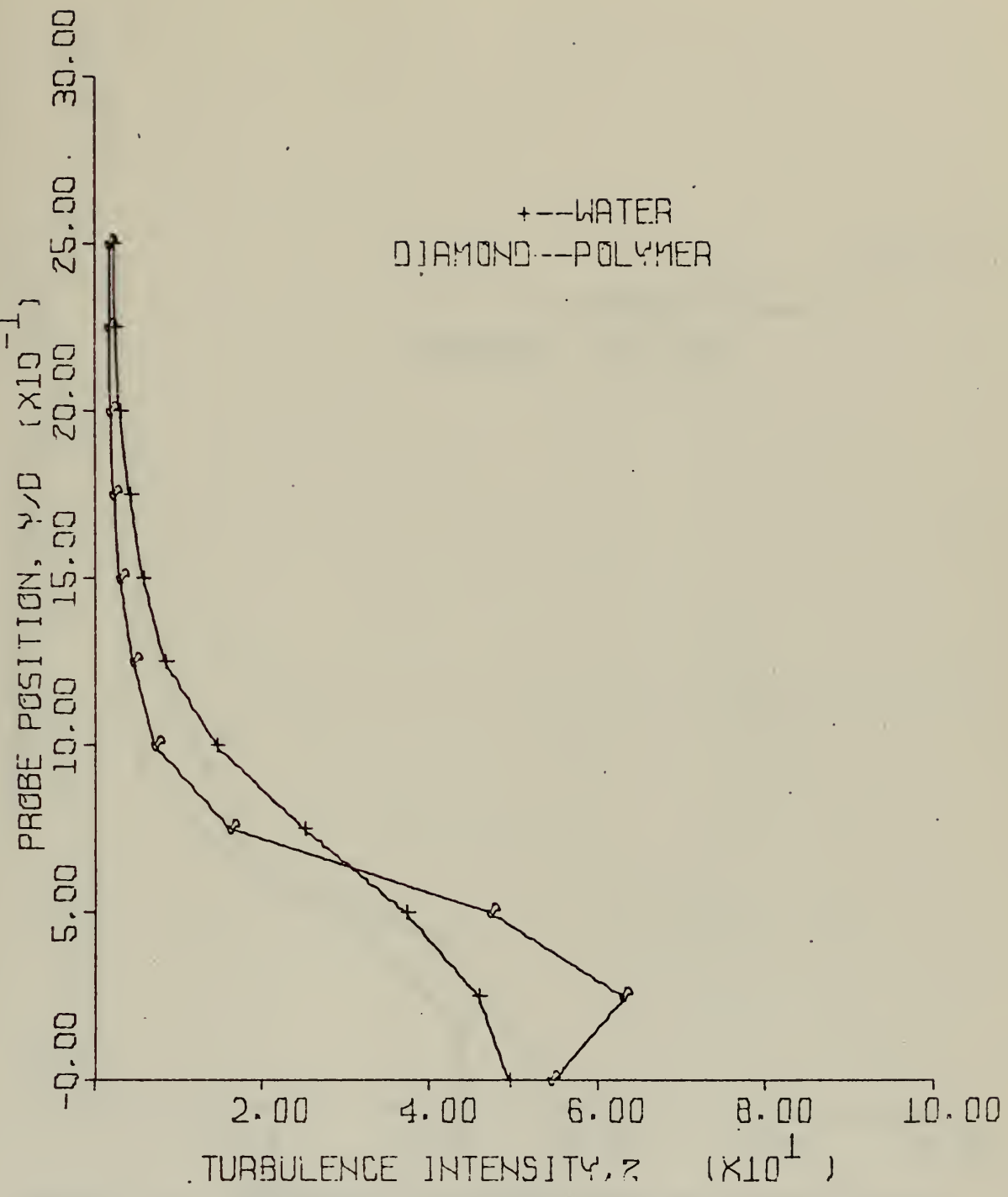

FIGURE 34: TURBULENCE INTENSITY PROFILES FOR TAP WATER AND 25 WPPM POLYMER SOLUTIONS; 20% PDR; RE = 80,000; X/D = 1.5

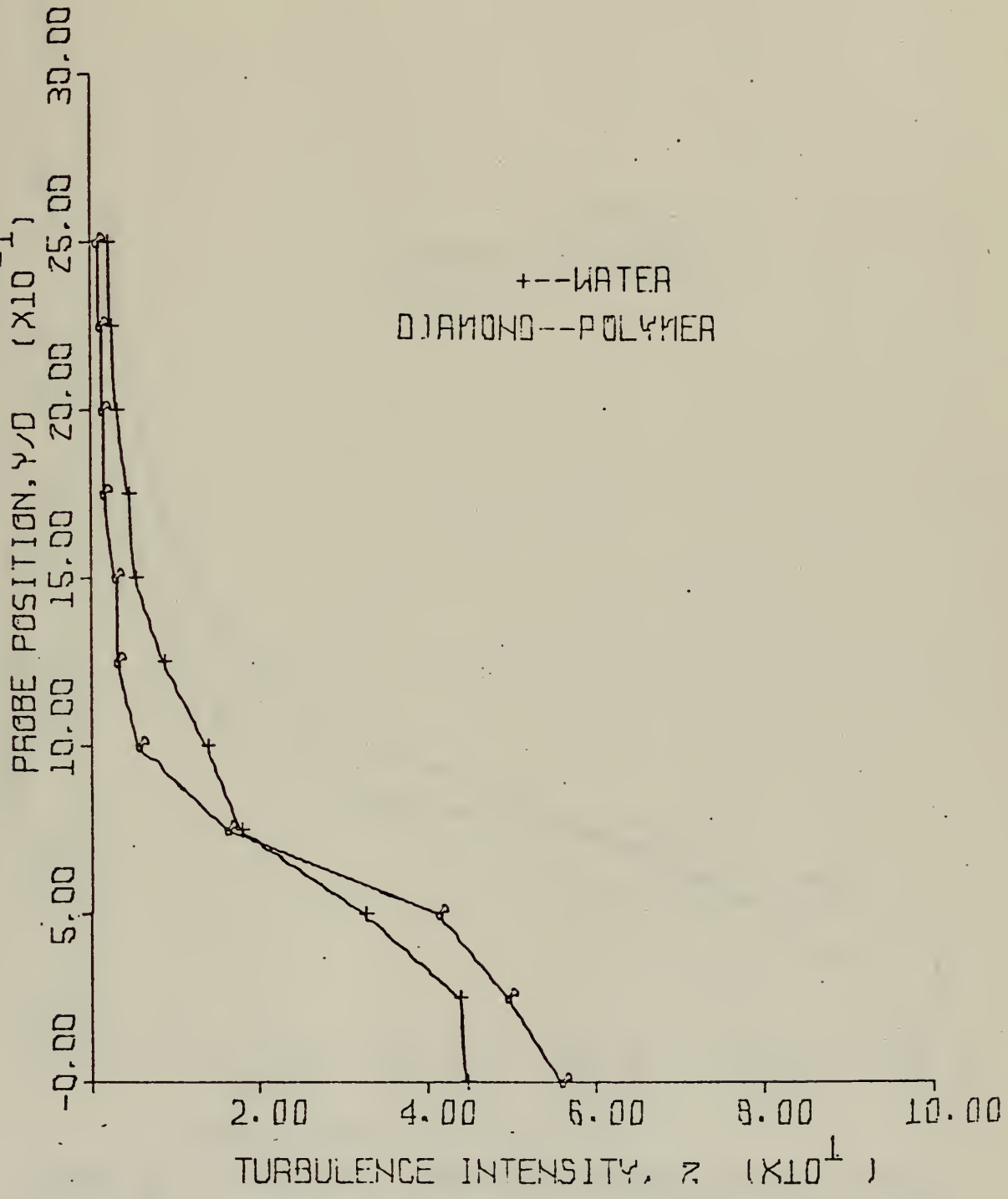

FIGURE 35: SCHIMMELS' TURBULENCE INTENSITY PROFILES FOR TAP WATER AND 25 WPPM POLYMER SOLUTIONS; 22% PDR; RE = 80,000; X/D = 1.5

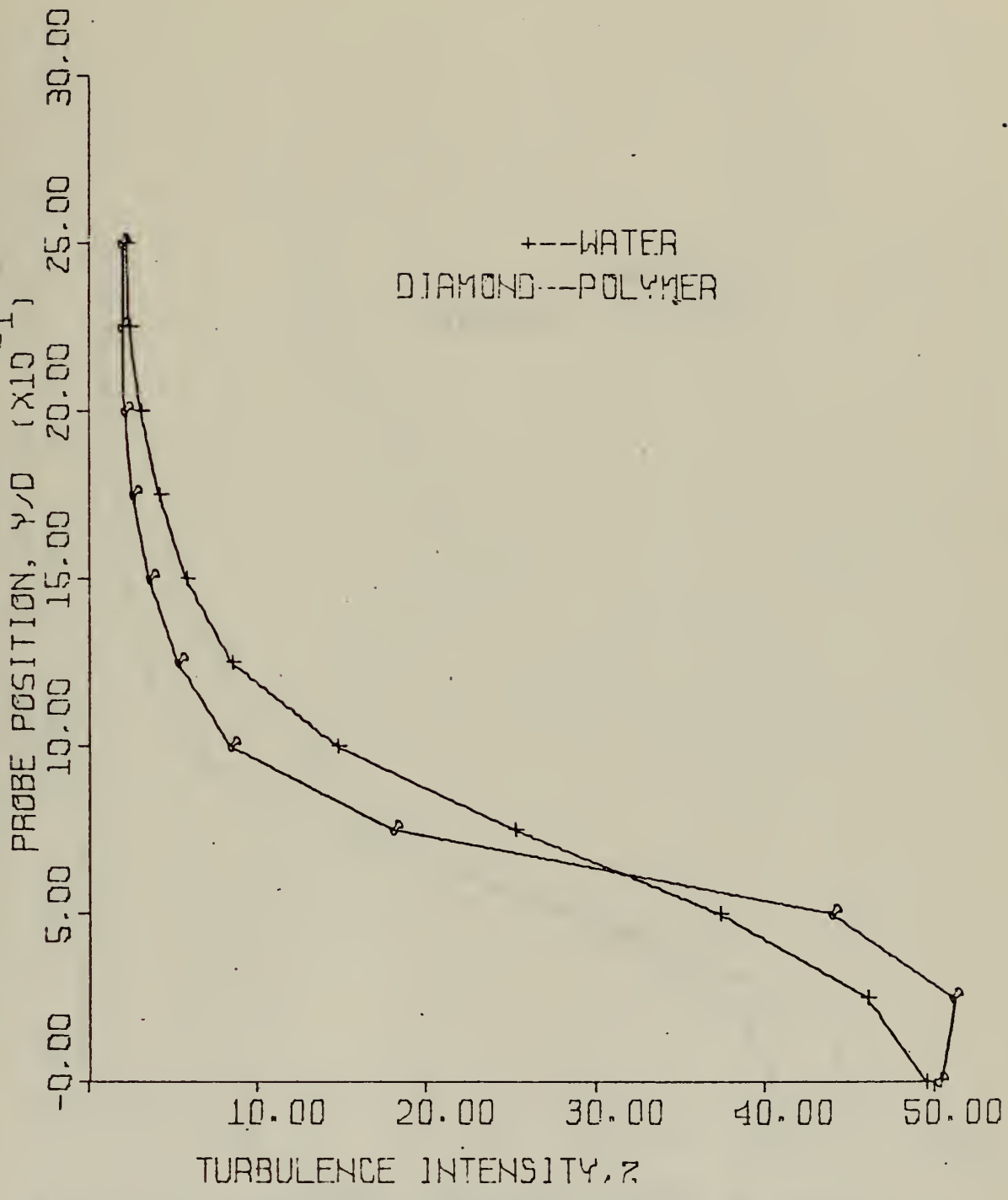

FIGURE 36: TURBULENCE INTENSITY PROFILES FOR TAP WATER AND 25 WPPM POLYMER SOLUTIONS; 2% PDR; RE = 80,000; X/D = 1.5

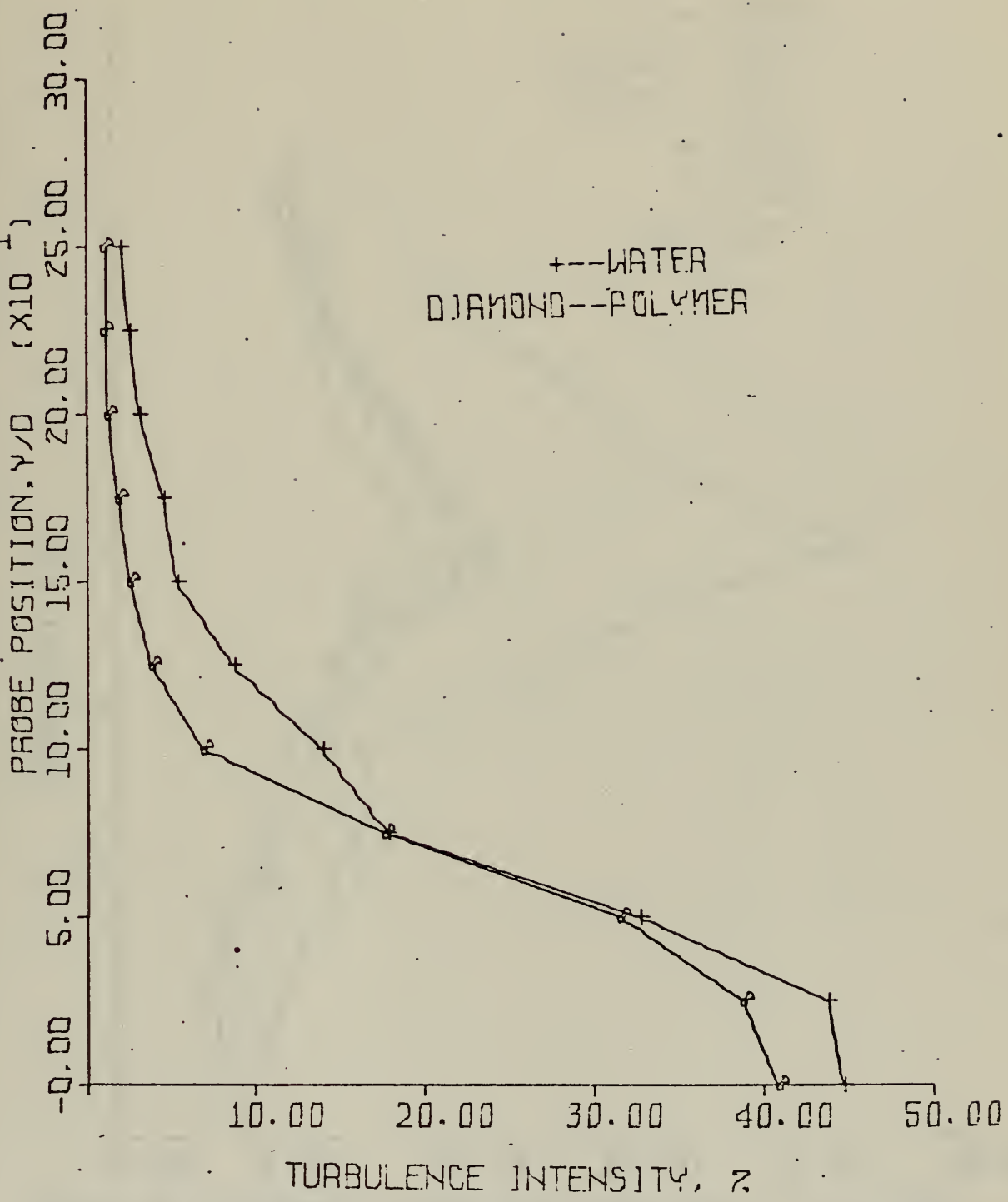

FIGURE 37: SCHIMMELS' TURBULENCE INTENSITY PROFILES FOR TAP WATER AND 25 WPPM POLYMER SOLUTIONS, 7% PDR; RE = 80,000; X/D = 1.5

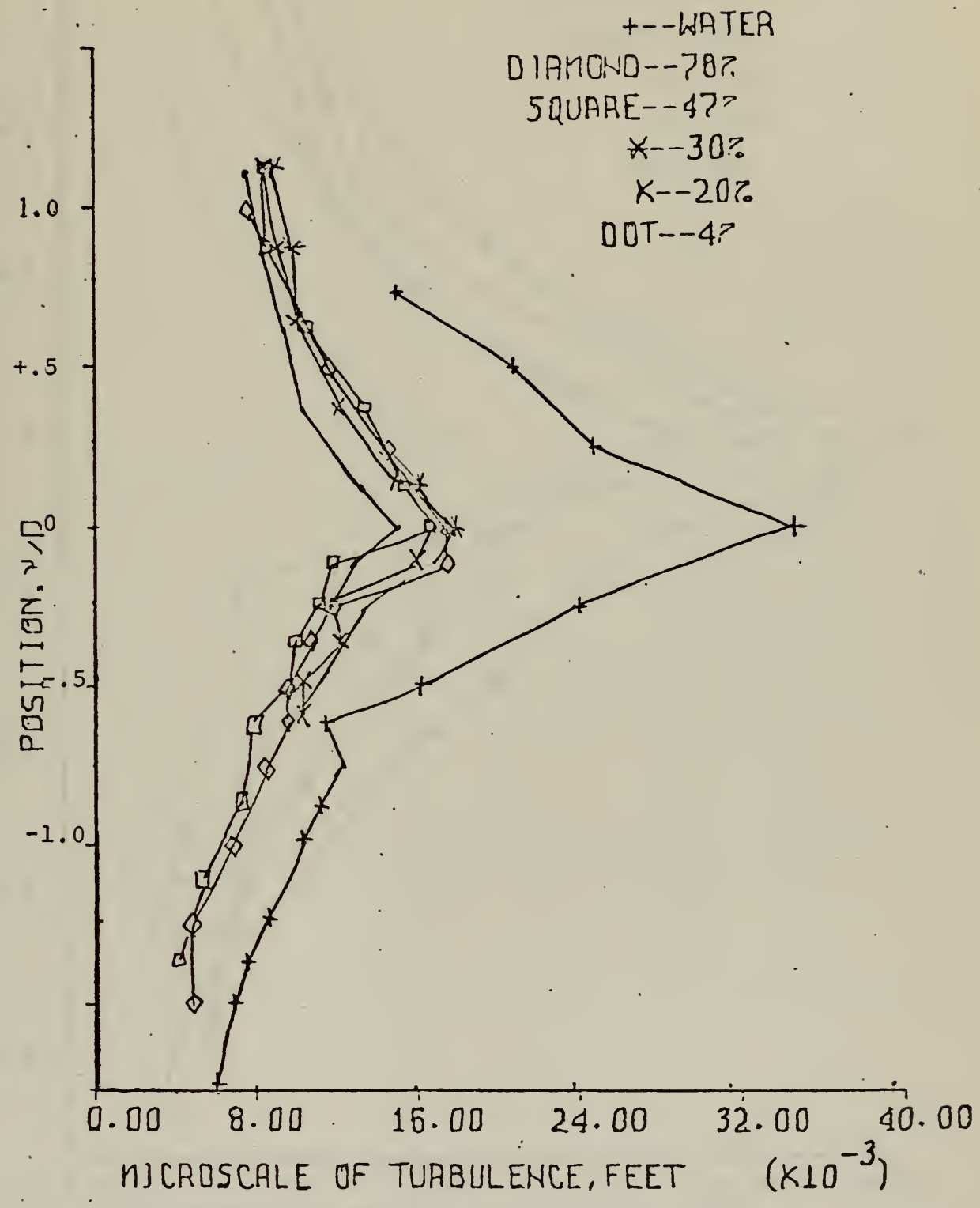

FIGURE 38: MICROSCALE OF TURBULENCE PROFILES WITH THE MAXIMUM VALUES ALIGNED AS THE REFERENCE POINT; RE = 100,000' X/D = 2.5

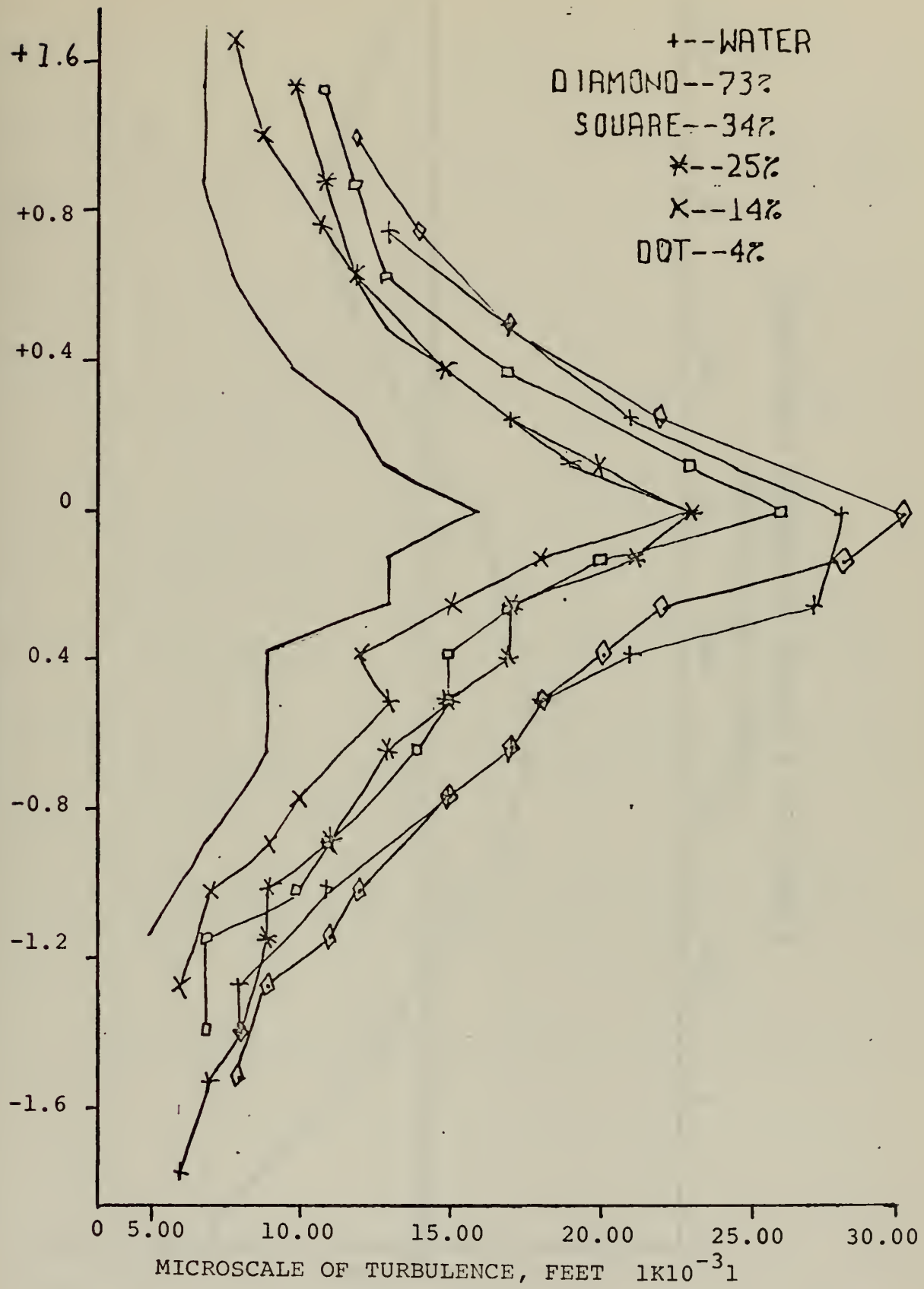

FIGURE 39: MICROSCALE OF TURBULENCE PROFILES WITH THE MAXIMUM VALUES ALIGNED AS THE REFERENCE POINT; RE = 140,000; X/D = 2.5

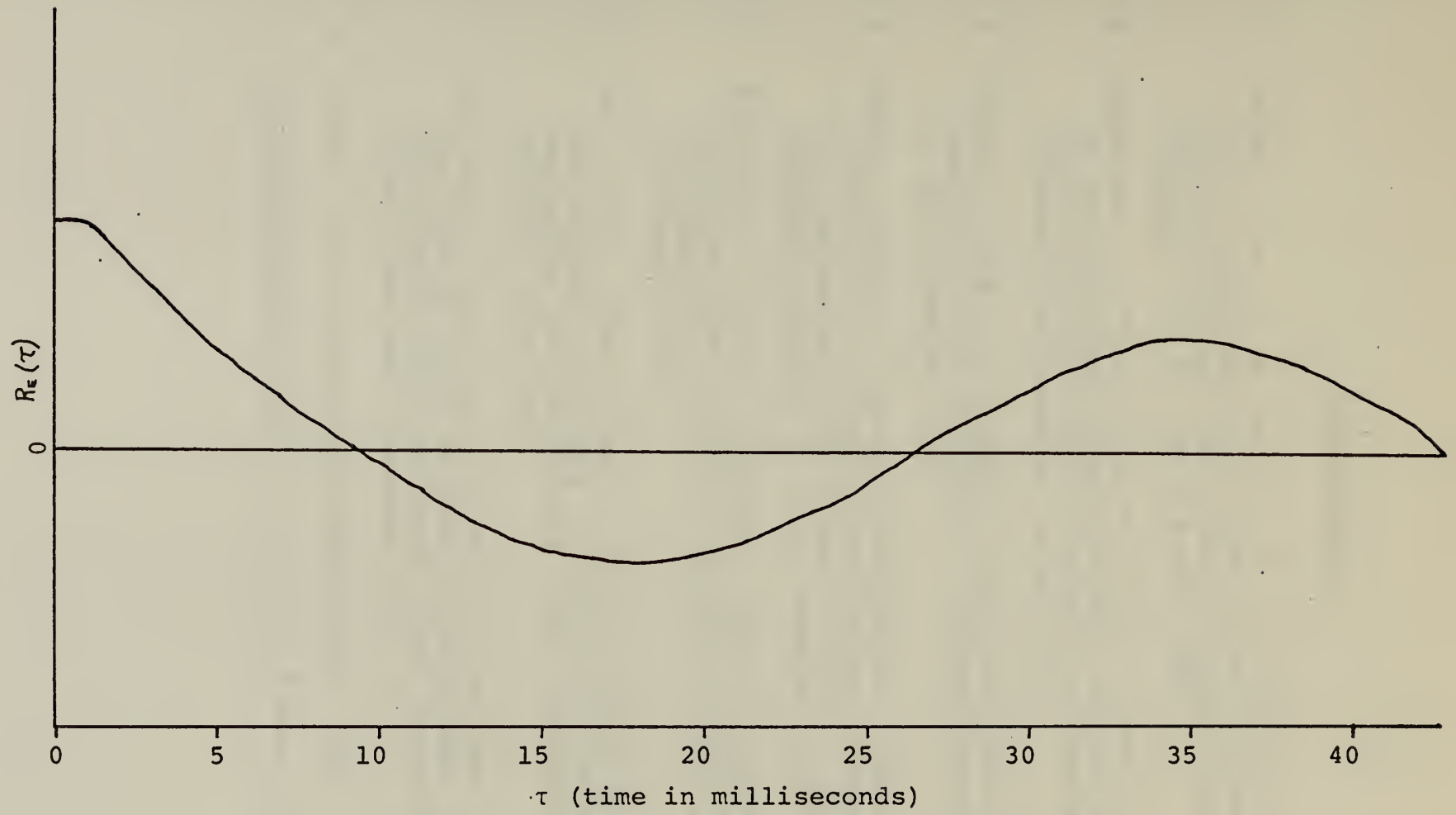

FIGURE 40: A TYPICAL MACROSCALE CORRELOGRAM

BIBLIOGRAPHY

1. Smith, K. A., E. W. Merrill, H. S. Mickley, and P. S. Virk, "Anomalous Pitot Tube and Hot-Film Measurements in Dilute Polymer Solutions," Chemical Engineering Science, Vol. 22, pp. 619-626, 1967.

2. Kowalski, T., "The Effect of Dilute Polymer Solutions on the Turbulence Characteristics and the Frictional Drag of External Flows," Doctoral Dissertation, University of Waterloo, March 1969.

3. Goren, Y. and J. F. Norbury, "Turbulence Flow of Dilute Aqueous Polymer Solutions," Transactions of ASME, p. 814, December 1967.

4. Lumley, John L., "The Toms Phenomenon: Anomalous Effects in Turbulent Flow of Dilute Solutions of High Molecular Weight Linear Polymer," Applied Mechanics Reviews, p. 1139, December 1967.

5. Sarpkaya, T. and P. G. Rainey, "Flow of Dilute Polymer Solutions about Circular Cylinders," Report Number: NPS-59SL1021A, Naval Postgraduate School, Monterey, 26 February 1971.

6. Kell, R. E., "The Effect of Dilute Polymer Solution on the Strouhal Frequency of Circular Cylinders," Mechanical Engineer Thesis, Naval Postgraduate School, Monterey, June 1971.

7. Schimmels, John Norman, "A Study of the Wake Region of the Flow of Dilute Polymer Solution About Circular Cylinders," Master's Thesis, Naval Postgraduate School, Monterey, December 1971.

8. Hinze, J. O., Turbulence, McGraw-Hill, 1959.

9. Viscous Drag Reduction, p. 281-295, Plenum Press, 1969.

INITIAL DISTRIBUTION LIST

		No. Copies
1.	Defense Documentation Center Cameron Station Alexandria, Virginia 22314	2
2.	Library, Code 0212 Naval Postgraduate School Monterey, California 93940	2
3.	Asst. Professor T. M. Houlihan, Code 59 Hm Department of Mechanical Engineering Naval Postgraduate School Monterey, California 93940	2
4.	LT. J. R. Fitts Staff, Commander Amphibious Force, Pacific San Diego, California 92155	1
5.	Department of Mechanical Engineering, Code 59 Naval Postgraduate School Monterey, California 93940	1

Security Classification

DOCUMENT CONTROL DATA - R & D

(Security classification of title, body of abstract and indexing annotation must be entered when the overall report is classified)

1. ORIGINATING ACTIVITY (Corporate author)	2a. REPORT SECURITY CLASSIFICATION
Naval Postgraduate School Monterey, California 93940	Unclassified
	2b. GROUP

3. REPORT TITLE

Turbulence Studies of the Flow of Dilute Polymer Solution about Circular Cylinders

4. DESCRIPTIVE NOTES (Type of report and, inclusive dates)

Master's Thesis; June 1972

5. AUTHOR(S) (First name, middle initial, last name)

Joel R. Fitts

6. REPORT DATE	7a. TOTAL NO. OF PAGES	7b. NO. OF REFS
June 1972	81	9

8a. CONTRACT OR GRANT NO.	9a. ORIGINATOR'S REPORT NUMBER(S)
b. PROJECT NO.	
c.	9b. OTHER REPORT NO(S) (Any other numbers that may be assigned this report)
d.	

10. DISTRIBUTION STATEMENT

Approved for public release; distribution unlimited.

11. SUPPLEMENTARY NOTES	12. SPONSORING MILITARY ACTIVITY
	Naval Postgraduate School Monterey, California 93940

13. ABSTRACT

This study was a continuation of previous investigations of the flow of dilute (25 WPPM) polymer (Polyox WSR-301) solutions about bluff bodies in the drag transition flow regime. Detailed measurements of turbulence intensity, and turbulence microscale were taken in the near wake region of a circular cylinder for several degradation states of polymer flow. Additionally, the effects of polymer degradation upon hot-film anemometer operations were determined. The results of this study substantiated the determinations on turbulence indices in polymer flows which were previously reported.

DD FORM 1 NOV 65 1473 (PAGE 1)

S/N 0101-807-6811

Security Classification

A-31408

14 KEY WORDS	LINK A		LINK B		LINK C	
	ROLE	WT	ROLE	WT	ROLE	WT
Polymer Flows						
Turbulence						
Hot-Film Anemometer						
Drag Reduction						

29 OCT 74 21915

Thesis 136741
F473 Fitts
c.1 Turbulence studies of the flow of dilute polymer solution about circular cylinders.

29 OCT 74 21915

Thesis 136741
F473 Fitts
c.1 Turbulence studies of the flow of dilute polymer solution about circular cylinders.

thesF473
Turbulence studies of the flow of dilute
3 2768 002 00204 0
DUDLEY KNOX LIBRARY